# Supplemental Online Content

Izumi D, Zhu Z, Chen Y, et al. Assessment of the diagnostic efficiency of a liquid biopsy assay for early detection of gastric cancer. *JAMA Netw Open.* 2021;4(8):e2121129. doi:10.1001/jamanetworkopen.2021.21129



© 2021 Izumi D et al. *JAMA Network Open.*

This supplemental material has been provided by the authors to give readers additional information about their work.

© 2021 Izumi D et al. *JAMA Network Open*.

## eMethods

### Study design and participants

We analyzed more than 1900 tissue and serum specimens from patients with GC, adjacent normal tissues and healthy participants in a four-phase study, which involved a biomarker discovery phase, a tissue validation phase, a retrospective serum validation phase, and a prospective serum performance evaluation phase (**Supplementary Figure 1**).

The biomarker discovery cohort (436 GC tissues and 41 adjacent normal mucosae from TCGA, consisting of small RNA-sequencing data and generated by the TCGA Research Network: https://www.cancer.gov/tcga) was analyzed to identify miRNA candidates for the early diagnosis of GC. Subsequently, miRNA expression profiles from two independent validation datasets, GSE23739 (40 GC tissues and 40 adjacent normal mucosae; validation dataset 1) and GSE33743 (37 GC tissues and 4 adjacent normal mucosae; validation dataset 2), were evaluated for the diagnostic performance of the discovered miRNA candidates. The data are accessible at NCBI GEO database (*32*).

During the tissue validation phase, qRT-PCR assays were performed to interrogate the expression levels of candidate miRNAs in 50 pairs of matched, fresh-frozen, primary tumor and adjacent normal tissues from patients with GC. These specimens were obtained from patients enrolled at Kumamoto University, Japan, who underwent curative resection without any pretreatment during 2014–2015. The matched corresponding normal tissues were collected from the greater curvature, and at least 5 cm away from the cancer tissue.

In the retrospective serum validation phase, two independent patient cohorts were analyzed, totaling 586 serum specimens. In the serum internal validation cohort, 216 serum specimens were collected from patients with GC and 43 specimens from endoscopically negative patients enrolled at Kumamoto University, Japan, between 2010 and 2015. Endoscopically negative patients were those who had esophagogastroduodenoscopy and diagnosed as negative for gastric cancer and had never diagnosed as any other cancer recruited at Kumamoto University. In the serum external validation

© 2021 Izumi D et al. *JAMA Network Open.*

cohort, sera were collected from 288 patients with GC and 39 serum specimens from healthy participants enrolled at Nagoya University, Japan, between 1997 and 2015. Healthy participants were randomly recruited at Nagoya University from people who have no diagnosed disease. In addition, the status of tumor markers, CEA and CA19-9, were also collected from the medical records of each institution. Written informed consent was obtained from all patients, and the institutional review boards of all participating institutions approved the study. In the serum validation phase, the three independent patient cohorts (TCGA, GSE23739, GSE33743) were analyzed again. Based on qRT-PCR data in serum, two miRNAs with low expression (miR-196a and miR-196b) and two others that were highly correlated with one another (miR-21 and miR-181a) were excluded from subsequent signature construction. The diagnostic potential of the initial signature was evaluated by performing a 5-fold cross-validation in our serum cohort (Kumamoto, n = 259) for internal validation, as well as an independent external validation cohort (Nagoya, n = 327). To further optimize a robust risk formula, a public dataset (GSE106817 cohort, data accessible at NCBI GEO database (*33*)) was used for miRNA expression profiling in sera from patients with GC and healthy participants. Using circulating miRNA expression profiles for all 115 patients with GC and a matched number of healthy participants (randomly selected from a larger cohort [n = 2759]), a 3-miRNA signature was developed using logistic regression and elastic net regularization, followed by establishment of a risk probability model. Public serum datasets were downloaded from GEO: GSE25609 (colorectal cancer, CRC), GSE85589 (pancreatic cancer, PC), GSE46729 (non-small cell lung cancer, NSCLC), GSE31309 (breast cancer, BC), and GSE31568 (ovarian cancer, OV). In each dataset, the miRNA expression values were Z-normalized.

In the prospective serum validation phase, serum specimens were collected from 176 patients with GC and 173 healthy participants, matched by age and sex, who were prospectively recruited from March 2017 to August 2018 at Affiliated Hospital of Jiangsu University and Nantong Tumor Hospital, Jiangsu, China (**Table 1**).

© 2021 Izumi D et al. *JAMA Network Open.*

## Prospective serum validation cohort

For prospective serum validation phase, patients who had a history of recurrent or other metastatic cancer were excluded from this study. Blood samples were taken when the patient was diagnosed with GC for the very first time without any treatment. Diagnosis was made by means of imaging techniques (computed tomography or magnetic resonance) and blood examination and verified by histopathological examination. All patients provided informed consent and met the inclusion criteria when enrolled in the study. CEA and CA19-9 levels were estimated in the serum specimens for patients with GC and healthy participants based on Cobase 601 (Roche Diagnostics) with Roche original reagents (ref. 11731629 and 11776193 respectively). Using qRT-PCR data for the 3-miRNA signature, the risk-scoring formula established in the previous cohort was applied and the performance of these circulating miRNA biomarkers was interrogated.

## Sample collection and processing

Whole blood was collected in the blood collection tube without clot activator and without anticoagulants and left at room temperature (15-25°C) until complete clotting. The serum was transferred to a new tube after centrifuging for several times. After the serum was separated from the whole blood, it was stored at -80°C immediately for further processing.

## Genome-wide miRNA data analysis

In the discovery phase, we first analyzed genome-wide miRNA sequencing data from TCGA (discovery cohort) to identify candidate miRNAs for the early detection of patients with GC. More specifically, level-3 miRNA expression data, including 436 tumors and 41 normal tissues, was downloaded from Firehose Broad GDAC portal (http://gdac.broadinstitute.org/, accessed on Nov 1, 2015). The miRNA expression levels, measured by reads per million miRNAs mapped (RPM), were

© 2021 Izumi D et al. *JAMA Network Open.*

first log2-transformed. Differential miRNA expression analysis was performed between GC and adjacent normal tissues using the bioconductor package and "limma" package in R (*34*). To further evaluate the predictive power of each miRNA's expression level in distinguishing GC from normal tissue, AUC was calculated. Among 1046 targets, 104 were differentially expressed (BH-adjusted $P <$ 0.05, absolute log2 fold change > 1 (*34*)) between GC and normal tissues. Among these, 9 miRNAs (miR-21, -196a-1, -146b, -196b, -135b, -181b, -181a, -93 and -335) were further selected based on the following criteria: BH-adjusted $P<1 \times 10^{-5}$, AUC > 0.9 and upregulated in GC. In addition, we also included two additional miRNAs, miR-196a-2 and 18a due to their high discriminative power (AUC=0.90 and 0.87, respectively), and because they were highly overexpressed in GC patients (log2 fold change >2, BH-adjusted $P < 1 \times 10^{-5}$). Due to the annotation differences between platforms, we combined expression data of miR-196a-1 and miR-196a-2 together as a single miRNA probe (miR-196a), which led to reduction of the 11-miRNA candidates to 10 miRNAs. 10 differentially expressed and discriminatory miRNAs between GC and normal tissues were selected as the initial signature candidates.

To confirm their diagnostic potential, the 10 miRNAs were validated in two additional independent datasets. GSE23739 included 40 GC and 40 non-cancerous tissue specimens with miRNA profiling data acquired using the Agilent-019118 Human miRNA Microarray platform (*35*). GSE33743 included 37 primary GC tissues and 4 normal gastric mucosa profiled for miRNA expression using the miRNAChip_human_V2 miRNA microarrays (National DNA-Microarray Facility) containing 1175 probes(*36*). The miRNA expression data was downloaded from GEO using Bioconductor package "GEOquery" in R, which was subsequently preprocessed using the methods described by Carvalho and colleagues (*35, 36*).

### miRNA-mRNA regulatory network interaction and functional analysis

A miRNA-mRNA network was constructed to study the functional significance of the candidate

© 2021 Izumi D et al. *JAMA Network Open.*

miRNAs. Specifically, for each miRNA, its downstream target mRNAs was identified based on two key criteria: first, that each miRNA-mRNA interaction had been experimentally validated based on the miRTarBase database (V8) (*21*); second, that each downstream mRNA was differentially expressed between tumor and normal samples (|log2 fold change| > 2 & BH-adjusted $P < 0.05$) in the TCGA dataset. The functional analysis was performed based on hypergeometric tests using the "clusterProfiler" package (*37*), with C2 (curated gene sets) and C5 (GO and KEGG gene sets) collections retrieved from the MSigDB Database (v7.0) (*38*). *P* values were corrected for multiple hypothesis testing using the BH procedure, and a BH-adjusted $P < 0.0001$ was considered statistically significant.

## Random Forest classification

To further evaluate the robustness of 10-miRNA signature across different datasets, a Random Forest classifier was trained using the expression levels of the 10 miRNAs by analyzing results from 41 GC and matched adjacent normal tissues in the discovery dataset. Z-normalization was performed for each miRNA separately in both validation datasets. Using the trained Random Forest classifier, predictive probabilities were calculated for identifying patients with GC, and the diagnostic performance of the combination of 10 miRNA candidates was assessed based on the AUC for both validation datasets.

## Cost-effectiveness analysis

CE analysis was performed under the following clinical assumptions **(Supplementary Table 11)**: Non-invasive screening was assumed to be performed on a high-risk population, Chinese men between ages 50–75 years old. The compliance rate was estimated to be approximately 45%. The test-positive group were assumed to go on to have a confirmatory test using endoscopy and biopsy. The biopsy test is considered the gold standard, with 100% sensitivity and specificity. The test-negative group were assumed to have a 3-year follow-up, during which cancer patients would be detected during the follow-up period. For the non-screening group, 10% of high-risk population were estimated to receive an

© 2021 Izumi D et al. *JAMA Network Open.*

endoscopy test to evaluate the incidence of cancer. Due to the high sensitivity and specificity of the 3-miRNA signature, the rate of early-stage patients diagnosed was estimated to rise. Using the miRNA test in a large-scale screening was estimated to increase the detection rate of early-stage GC, which is calculated from the sensitivity and specificity of the 3-miRNA signature under the assumed compliance rate.

For the assumption of cancer treatment, early or advanced stages of GC (TNM Stage 1–3) were considered curable and would be cured after two years with a stage-specific recurrence rate. For cured patients, we estimated they would have additional medical expenditure (1000 CNY or 142.6 USD) every year before recurrence. Terminal stage GC (TNM Stage 4) was considered as untreatable, with only palliative care, and patients were assumed to die after one year. Considering the prognosis following cancer recurrence is poor, all relapsed patients were assumed to have Stage 4 status. Cost and incidence rate were either collected from the literature or estimated based on in-house clinical records**.**

## RNA isolation and qRT-PCR

miRNA extraction from tissue specimens was performed using miRNeasy RNA isolation kits (Qiagen, Valencia, California, USA), whereas miRNA extraction from serum was performed using miRNeasy serum/plasma kits (Qiagen). TaqMan miRNA real-time qRT-PCR assays (Applied Biosystems, Foster City, California, USA) were used to detect and quantify miRNA expression. The expression levels of serum or tissue miRNAs were normalized against miR-16 and U6 expression levels, respectively, and results were calculated using the ΔCt method as previously described (*39*). To ensure consistent measurements throughout all assays, for each PCR amplification reaction, three independent RNA samples were loaded as internal controls to account for potential plate-to-plate variation, and the results from each plate were normalized against the internal normalization controls. All experiments were triplicated.

© 2021 Izumi D et al. *JAMA Network Open.*

Total RNA enriched in small RNAs was purified from serum samples using the miRNeasy Serum/Plasma Kit (Qiagen). C. elegans miR-39 miRNA mimic (miRNeasy Serum/Plasma Spike-In Control, Qiagen) was mixed thoroughly into all samples during the RNA isolation procedures for normalization of sample-to-sample variation. RNA extracted from serum samples was reverse-transcribed using a TaqMan MicroRNA Reverse Transcription Kit (Applied Biosystems) for subsequent qRT-PCR assays. qRT- PCR was performed using a TaqMan MicroRNA Assay kit and TaqMan Universal Master Mix II, no UNG (Applied Biosystems) through QuantStudioTM 7 Flex Real-Time PCR System (Applied Biosystems). The expression of miRNAs was normalized against the average expression level of miR-16 and 423-5p (Applied Biosystems) in all serum samples. Whenever we used kits from companies, we followed the instruction from the manufactures.

### Logistic regression analysis with elastic net regularization

Using 115 patients with GC and 115 healthy participants enrolled in the public serum cohort (GSE106817), we developed a 3-circulating-miRNA signature using logistic regression with elastic net regularization. Using the established risk scoring formula, we calculated risk probabilities for samples in the prospective serum cohort to evaluate the diagnostic performance.

### Statistical analysis

All statistical analyses were performed using Medcalc V.12.3.0 (Broekstraat 52, 9030; Mariakerke, Belgium), GraphPad Prism V5.0 (GraphPad Software, San Diego, California, USA), and R (3.3.3, R Development Core Team, https://cran.r-project.org/). Differential miRNA expression analysis was performed using the ‘limma’ package in R, and the resulting *P* values were adjusted using Benjamini-Hochberg’s method. Wilcoxon’s signed-rank test, the Mann-Whitney U test, and the Kruskal-Wallis test were used to analyze miRNA expression data obtained from qRT-PCR experiments, and results were expressed as mean ± standard error. Silhouette width was calculated using R package ‘cluster’

© 2021 Izumi D et al. *JAMA Network Open.*

with Euclidean distance. Pearson correlation coefficient was calculated by R package ‘stats’ and graphically displayed by R package ‘corrplot’. The principal components analysis and other statistical analyses including logistic regression were also performed using the “stats” package in R. AUCs derived from ROC curves were calculated with CIs using the “pROC” package in R; ROC curves were compared using DeLong’s test in the pROC package. The 10-miRNA Random Forest classifier was trained using the “caret” package in R. Logistic regression with elastic net regularization was performed using the “glmnet” package through the caret package in R, with default configuration of optimization. ORs were calculated using the “vcd” package in R.

© 2021 Izumi D et al. *JAMA Network Open*.

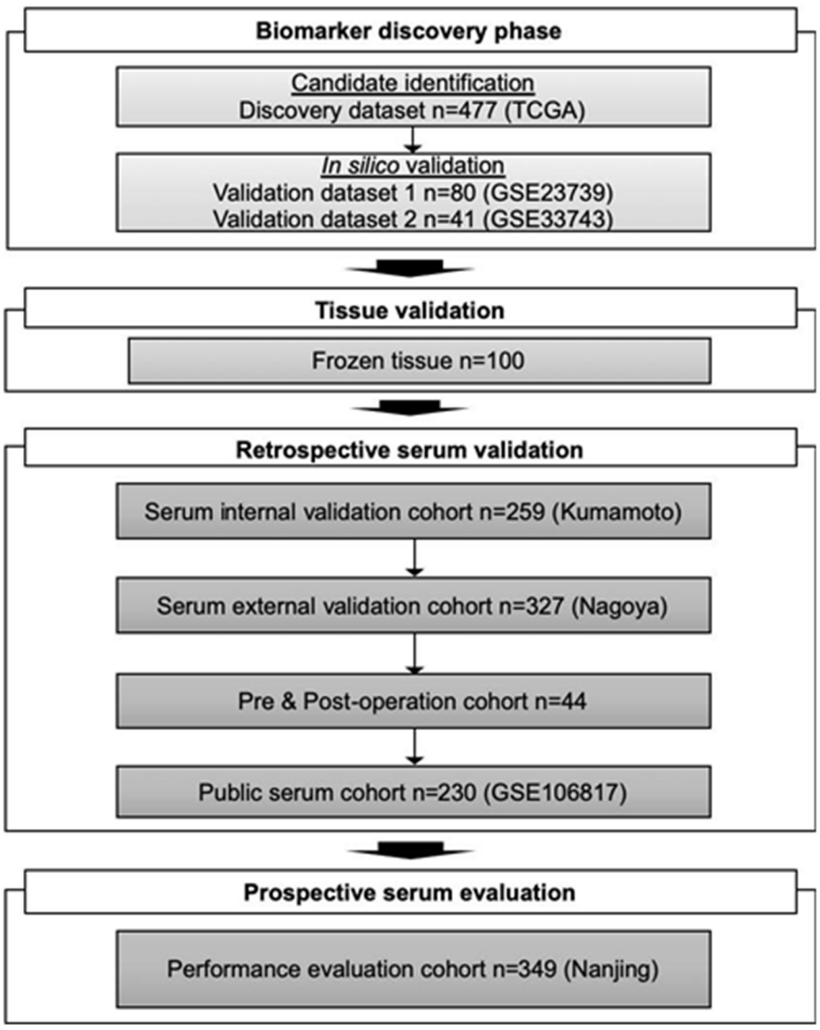


eFigure 1. Study design for the identification of a circulating miRNA expression signature for early detection of GC.

© 2021 Izumi D et al. *JAMA Network Open.*

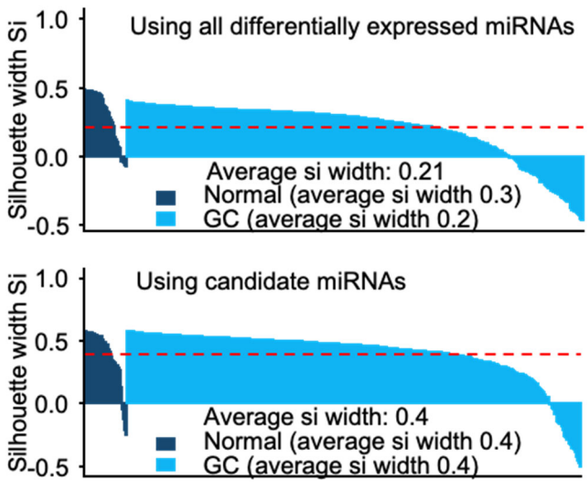


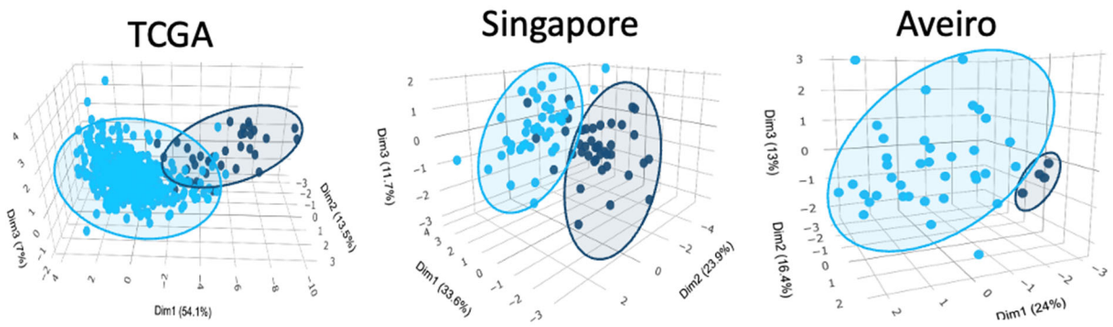


eFigure 2. Genome-wide discovery of miRNA candidates for GC diagnosis. (A) Using all differentially expressed miRNAs and 10 selected miRNAs, Silhouette analysis shows stability and consistency within GC and normal groups. Red dash line indicates the average silhouette width. (B) Principle component analysis shows 10 miRNAs can discriminate GC and normal samples.

© 2021 Izumi D et al. *JAMA Network Open.*

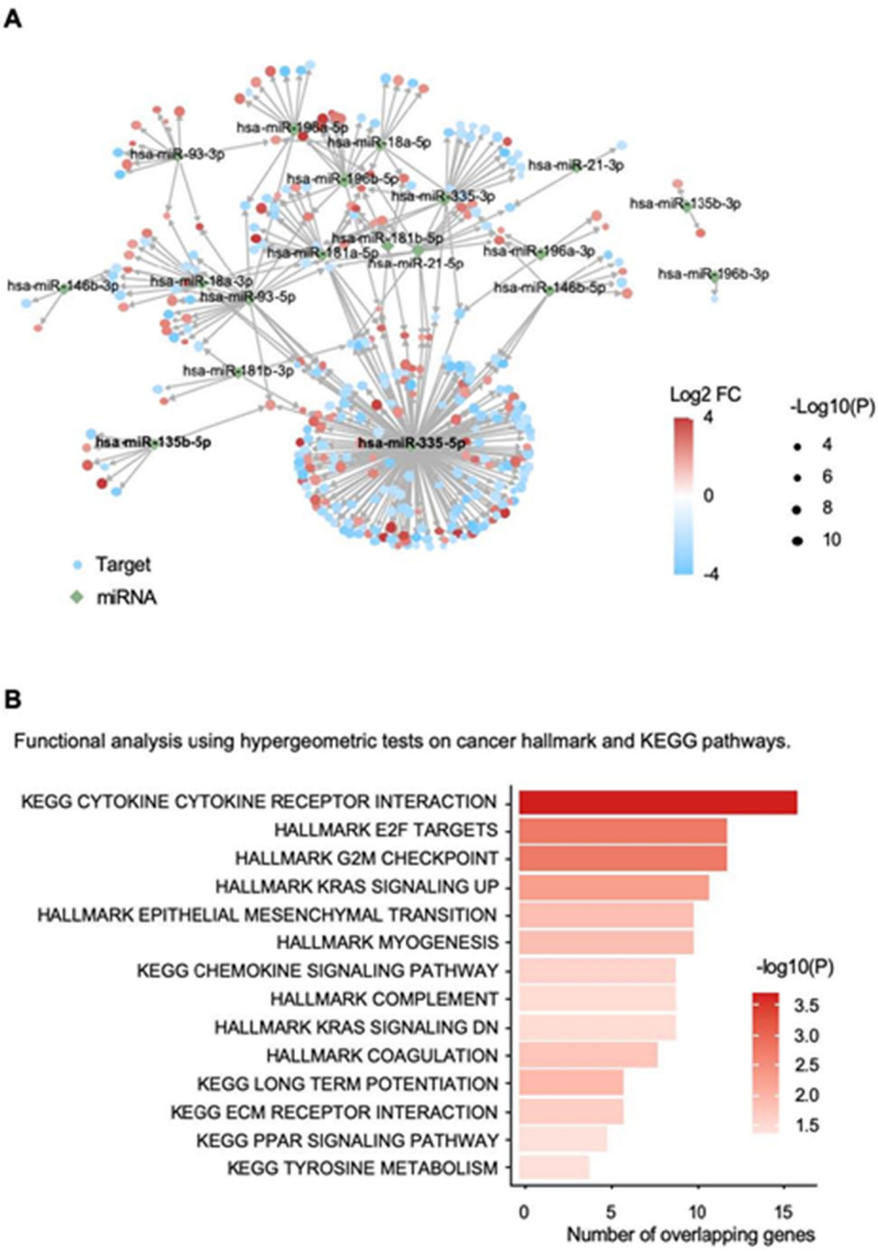


eFigure 3. miRNA regulatory network analysis and functional analysis of the miRNA target genes. (A) A regulatory network constructed using experimentally validated miRNA-mRNA interactions from miRTarBase (V8). Node size indicates the -log10 transformed BH-adjusted *P*, and color indicates the log2 fold change between GC and normal samples in the TCGA dataset. (B) Functional analysis using hypergeometric tests on cancer hallmark and KEGG pathways. The significantly enriched signaling pathways (BH-adjusted $P < 0.05$) are illustrated in the bar plot. Bar length indicates the number of overlapping genes and color indicates the *P* value.

© 2021 Izumi D et al. *JAMA Network Open.*

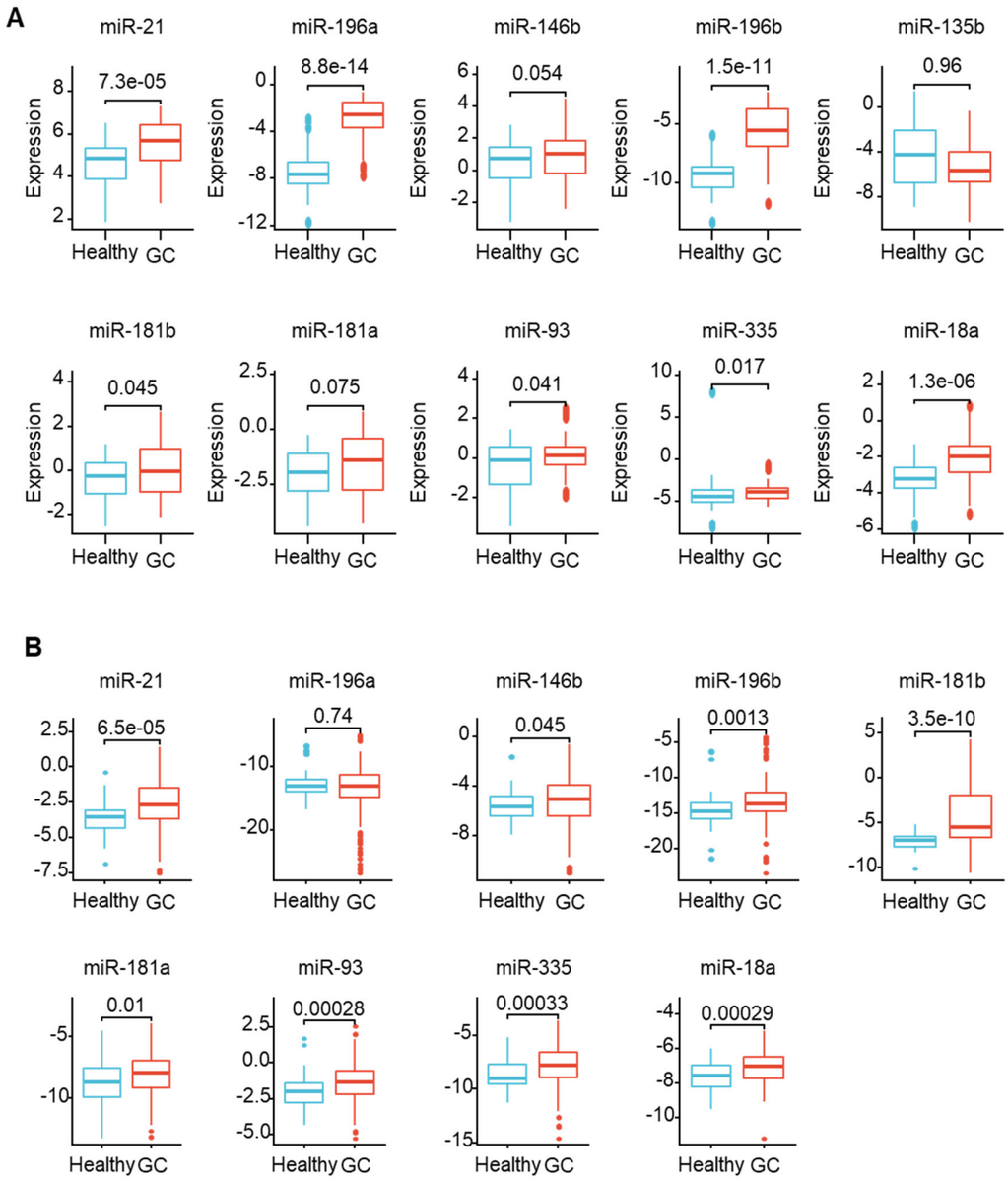


eFigure 4. Tissue validation and serum validation for the 10 miRNA candidates. (A) Boxplots with one-tailed Wilcoxon signed-rank tests comparing the expression levels between GC and adjacent healthy tissues. (B) Boxplots with Mann-Whitney U tests comparing the expression levels of the circulating miRNAs between patients with GC and healthy participants (Kumamoto cohort).

© 2021 Izumi D et al. *JAMA Network Open.*

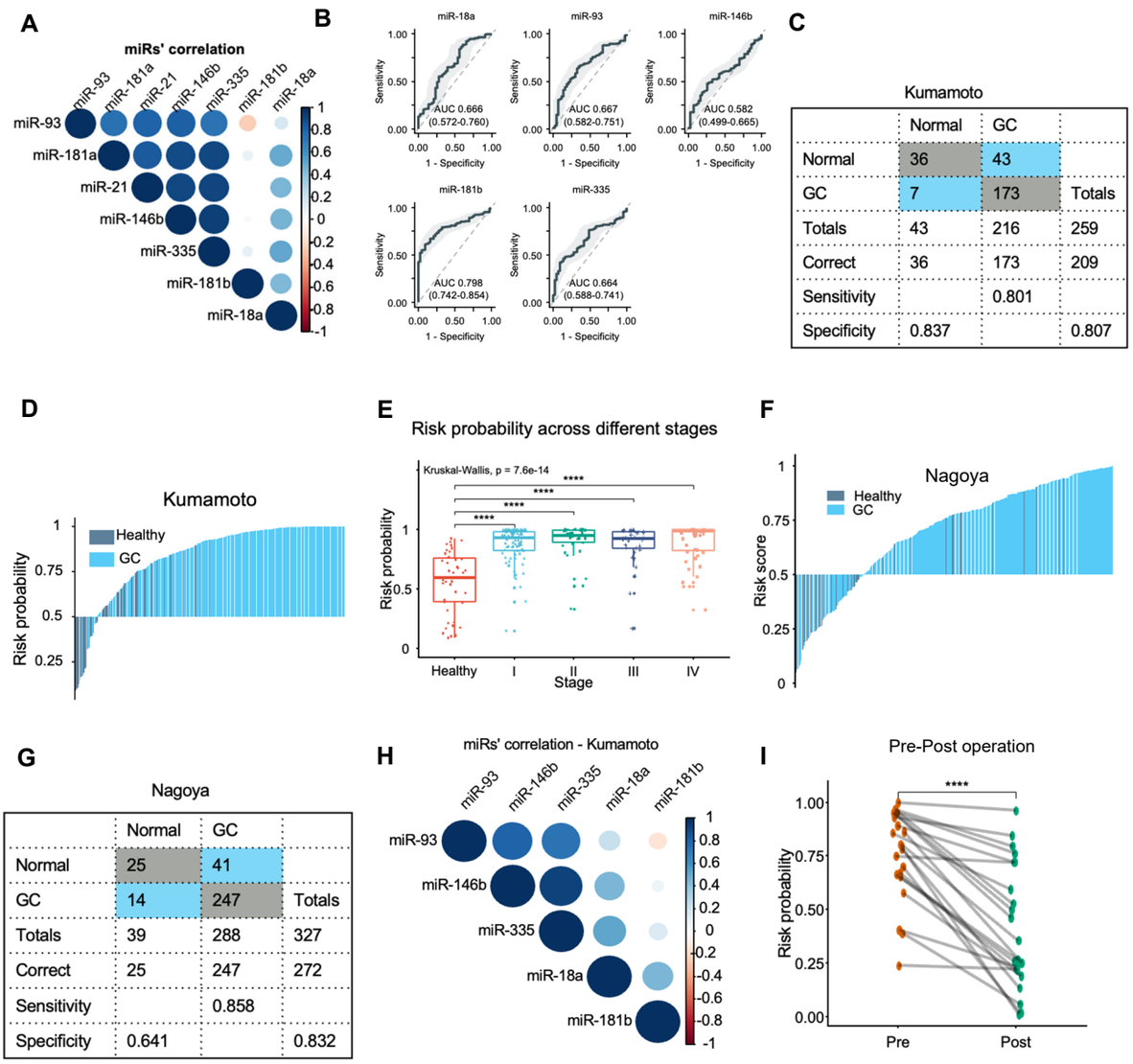


eFigure 5. Validation of the 5 circulating miRNAs in the Kumamoto cohort. (A) Correlation matrix of expression of seven miRNAs (miR-93, miR-181a, miR-21, miR-146b, miR-335, miR-181b and miR-18a) in the Kumamoto cohort. (B) ROC curves illustrating the diagnostic values of individual circulating miRNAs in differentiating patients with GC from healthy participants (Kumamoto cohort). (E) Confusion matrices built from diagnostic model prediction in the Kumamoto cohort. (D) Waterfall plot illustrating the detailed classification of patients with GC and participants using risk by risk probability in the Kumamoto cohort. (E) Boxplots comparing risk scores between patients with GC of different stages and healthy participants in the Kumamoto cohort. (F) Waterfall plot illustrating patients with GC and healthy participants ranked by risk probability in the serum external validation cohort (Nagoya). (G) Confusion matrices built from diagnostic model prediction in the Nagoya cohort. (H) Correlation matrix of expression of five miRNAs (miR-93, miR-146b, miR-335, miR-18a and miR-181b) in the Kumamoto cohort. (I ) Paired dot plots comparing risk scores calculated for 22 pairs of pre- and post-operative sera form patients with GC. A significant drop in GC risk was observed after curative surgery ($P < 0.0001$, Wilcoxon signed-rank test), suggesting that expression of the circulating miRNAs was derived from GC tissues.

© 2021 Izumi D et al. *JAMA Network Open.*

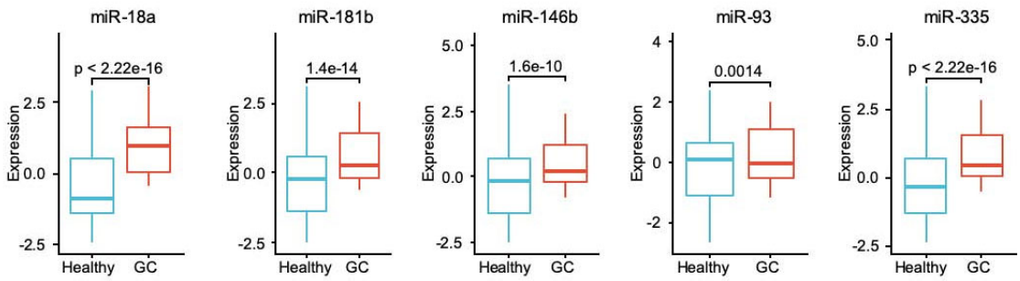


eFigure 6. Validation of the 5 circulating miRNAs in a public serum cohort (GSE106817). Boxplots with one-tailed Wilcoxon signed-rank tests comparing the expression levels of the circulating miRNAs between patients with GC and healthy participants.

© 2021 Izumi D et al. *JAMA Network Open.*

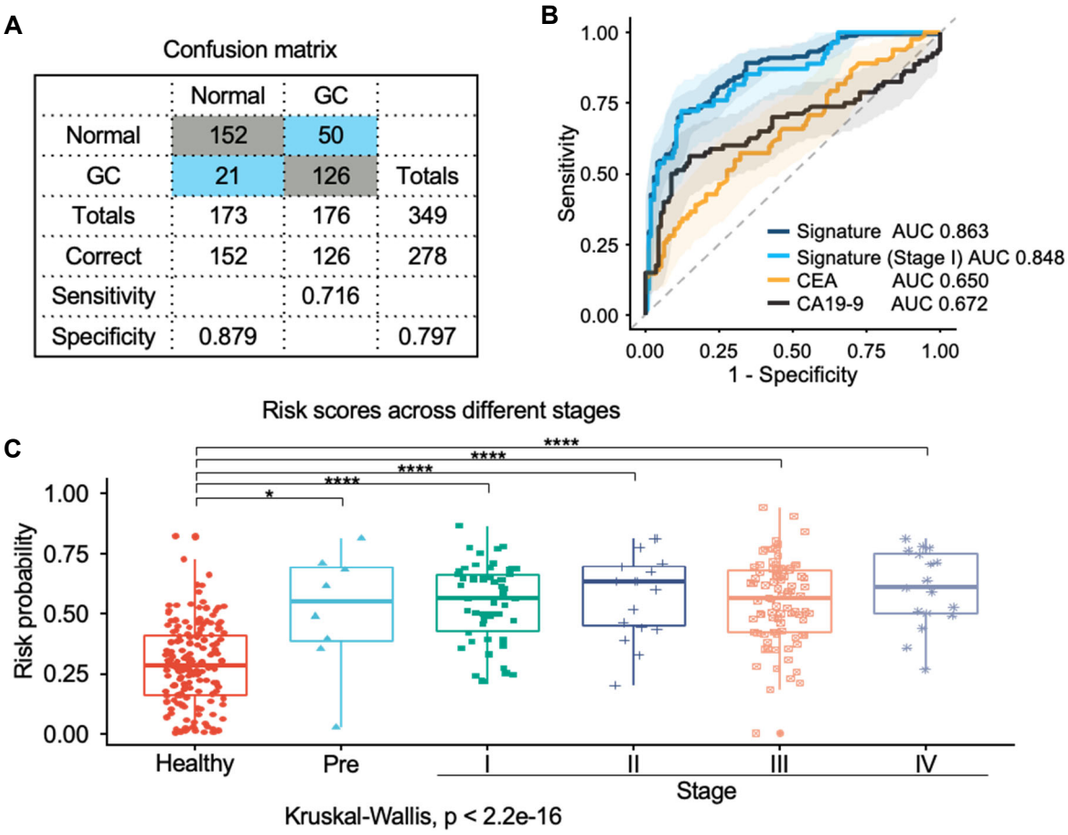


eFigure 7. Establishment of a 3-circulating-miRNA signature and evaluation in a prospective validation serum cohort. (A) Confusion matrices built from the diagnostic model prediction in the prospective validation cohort. (B) ROC curves demonstrating diagnostic performance of the 3-miRNA signature in all-stage GC samples, stage I GC samples, CEA and CA19-9 in a prospective validation cohort (Nanjing). ROC curves are shown with 95% CI (DeLong's test). (C) Boxplots comparing risk scores between patients with GC of different stages, precancerous lesion (pre) and healthy participants. All ROC curves are shown with 95% CI. The 95% CI of sensitivity and specificity (green line) for each miRNA is also shown at the best threshold (green point).

© 2021 Izumi D et al. *JAMA Network Open.*

**eTable 1.** Statistical summary of the initially identified 11 miRNAs from the discovery dataset

| miRNA | AUC | SEN | SPE | PPV | NPV | aveTumor | aveNormal | log2FC | *P* value | FDR-adjusted *P* value |
|---|---|---|---|---|---|---|---|---|---|---|
| hsa-mir-21 | 0.99 | 0.90 | 1.00 | 1.00 | 0.48 | 18.02 | 15.57 | 2.44 | 3.66E-25 | 3.19E-22 |
| hsa-mir-196a-1 | 0.94 | 0.95 | 0.81 | 0.98 | 0.60 | 6.63 | 1.89 | 4.73 | 9.26E-21 | 8.05E-18 |
| hsa-mir-146b | 0.92 | 0.91 | 0.76 | 0.98 | 0.44 | 9.38 | 6.97 | 2.42 | 2.41E-19 | 2.09E-16 |
| hsa-mir-196b | 0.91 | 0.80 | 0.90 | 0.99 | 0.30 | 7.66 | 3.15 | 4.51 | 4.98E-18 | 4.31E-15 |
| hsa-mir-135b | 0.91 | 0.74 | 0.95 | 0.99 | 0.26 | 5.35 | 2.16 | 3.19 | 7.26E-18 | 6.29E-15 |
| hsa-mir-181b-1 | 0.91 | 0.81 | 0.88 | 0.99 | 0.30 | 7.78 | 6.23 | 1.55 | 7.53E-18 | 6.51E-15 |
| hsa-mir-181a-1 | 0.90 | 0.83 | 0.83 | 0.98 | 0.31 | 10.02 | 8.54 | 1.48 | 9.75E-18 | 8.41E-15 |
| hsa-mir-93 | 0.90 | 0.73 | 1.00 | 1.00 | 0.26 | 12.28 | 10.50 | 1.78 | 1.68E-17 | 1.44E-14 |
| hsa-mir-335 | 0.90 | 0.79 | 0.90 | 0.99 | 0.29 | 6.43 | 4.39 | 2.04 | 1.96E-17 | 1.68E-14 |
| hsa-mir-196a-2 | 0.90 | 0.85 | 0.83 | 0.98 | 0.34 | 3.02 | 0.51 | 2.51 | 2.63E-17 | 2.25E-14 |
| hsa-mir-18a | 0.87 | 0.67 | 0.90 | 0.99 | 0.21 | 4.85 | 2.76 | 2.09 | 1.01E-14 | 8.56E-12 |

AUC, area under the ROC curve. SEN, sensitivity. SPE, specificit. PPV, positive predictive value. NPV, negative predictive value. ave, average. FC, fold change

© 2021 Izumi D et al. *JAMA Network Open.*

**eTable 2.** MiRNA-mRNA interactions in the regulatory network

| miRNA | miRTarBase ID | Target Gene | log2FC | BH-adjusted *P* value |
|---|---|---|---|---|
| hsa-miR-21-5p | MIRT000171 | NCAPG | 2.38 | 3.79E-16 |
| hsa-miR-181b-5p | MIRT000240 | CDX2 | 3.11 | 2.78E-05 |
| hsa-miR-181a-5p | MIRT000245 | CDX2 | 3.11 | 2.78E-05 |
| hsa-miR-21-5p | MIRT002416 | BTG2 | -2.01 | 4.03E-23 |
| hsa-miR-196a-5p | MIRT002942 | HOXC8 | 4.04 | 8.00E-14 |
| hsa-miR-181b-5p | MIRT003035 | GRIA2 | -2.59 | 2.16E-09 |
| hsa-miR-21-5p | MIRT003567 | SERPINB5 | 2.02 | 8.38E-04 |
| hsa-miR-135b-5p | MIRT003594 | IBSP | 4.24 | 1.00E-21 |
| hsa-miR-18a-5p | MIRT004387 | TNFSF11 | 2.76 | 5.71E-14 |
| hsa-miR-196b-5p | MIRT004638 | HOXC8 | 4.04 | 8.00E-14 |
| hsa-miR-146b-5p | MIRT005371 | KIT | -2.18 | 3.91E-15 |
| hsa-miR-335-5p | MIRT006110 | TFF2 | -2.26 | 2.56E-03 |
| hsa-miR-196a-5p | MIRT006803 | HMGA2 | 2.93 | 3.84E-07 |
| hsa-miR-335-5p | MIRT007304 | BIRC5 | 2.24 | 3.78E-13 |
| hsa-miR-335-5p | MIRT016709 | NPY | -3.29 | 3.33E-12 |
| hsa-miR-335-5p | MIRT016712 | USH1C | 2.08 | 5.20E-07 |
| hsa-miR-335-5p | MIRT016727 | DNASE1L3 | -2.71 | 2.37E-16 |
| hsa-miR-335-5p | MIRT016748 | SYNPO2 | -3.13 | 4.96E-14 |
| hsa-miR-335-5p | MIRT016769 | CCL15 | 2.52 | 3.58E-06 |
| hsa-miR-335-5p | MIRT016828 | LRP1B | -2.15 | 3.21E-09 |
| hsa-miR-335-5p | MIRT016831 | PRKN | -2.13 | 1.60E-20 |
| hsa-miR-335-5p | MIRT016848 | WNT7B | 3.49 | 2.69E-07 |
| hsa-miR-335-5p | MIRT016852 | F10 | -2.26 | 2.73E-12 |
| hsa-miR-335-5p | MIRT016866 | SPP1 | 3.09 | 1.75E-07 |
| hsa-miR-335-5p | MIRT016876 | MAPK4 | -3.60 | 5.61E-14 |
| hsa-miR-335-5p | MIRT016899 | SORBS2 | -2.00 | 1.55E-13 |
| hsa-miR-335-5p | MIRT016901 | NEFM | -2.58 | 9.17E-14 |
| hsa-miR-335-5p | MIRT016917 | HTR7 | -2.21 | 8.12E-15 |
| hsa-miR-335-5p | MIRT016925 | TUSC5 | -3.75 | 4.86E-18 |
| hsa-miR-335-5p | MIRT016935 | SALL4 | 4.04 | 2.35E-12 |
| hsa-miR-335-5p | MIRT016944 | CXCL9 | 2.49 | 2.08E-06 |
| hsa-miR-335-5p | MIRT016951 | VIP | -3.49 | 1.63E-12 |
| hsa-miR-335-5p | MIRT016968 | NECAB1 | -2.21 | 1.17E-12 |
| hsa-miR-335-5p | MIRT016993 | GRB7 | 2.35 | 6.71E-08 |
| hsa-miR-335-5p | MIRT017035 | CYP19A1 | 2.27 | 3.06E-09 |
| hsa-miR-335-5p | MIRT017058 | ASB11 | -2.38 | 9.34E-11 |
| hsa-miR-335-5p | MIRT017063 | SLC2A12 | -2.16 | 1.17E-12 |
| hsa-miR-335-5p | MIRT017068 | HSPB3 | -3.14 | 6.55E-13 |
| hsa-miR-335-5p | MIRT017072 | HOXA11 | 4.96 | 6.38E-11 |
| hsa-miR-335-5p | MIRT017114 | FLG2 | -2.20 | 1.23E-09 |
| hsa-miR-335-5p | MIRT017120 | FOXA2 | 2.13 | 6.15E-05 |
| hsa-miR-335-5p | MIRT017127 | C6orf223 | 3.11 | 3.65E-07 |

© 2021 Izumi D et al. *JAMA Network Open.*

| | | | | |
|---|---|---|---|---|
| hsa-miR-335-5p | MIRT017144 | HOXC6 | 2.54 | 5.00E-09 |
| hsa-miR-335-5p | MIRT017145 | MMRN1 | -2.86 | 1.31E-18 |
| hsa-miR-335-5p | MIRT017148 | WIF1 | -3.90 | 1.76E-15 |
| hsa-miR-335-5p | MIRT017159 | SFRP1 | -4.23 | 2.09E-25 |
| hsa-miR-335-5p | MIRT017193 | CPNE6 | -2.84 | 9.58E-13 |
| hsa-miR-335-5p | MIRT017225 | PYGM | -3.05 | 7.10E-24 |
| hsa-miR-335-5p | MIRT017231 | SLC27A6 | -2.62 | 2.81E-11 |
| hsa-miR-335-5p | MIRT017241 | IYD | 2.57 | 2.42E-05 |
| hsa-miR-335-5p | MIRT017263 | ILDR1 | 2.71 | 4.38E-15 |
| hsa-miR-335-5p | MIRT017272 | SERPINB5 | 2.02 | 8.38E-04 |
| hsa-miR-335-5p | MIRT017286 | PLA2G7 | 2.82 | 6.83E-15 |
| hsa-miR-335-5p | MIRT017304 | PGM5 | -3.67 | 9.10E-23 |
| hsa-miR-335-5p | MIRT017308 | IGSF10 | -2.16 | 2.67E-10 |
| hsa-miR-335-5p | MIRT017316 | GRIN2D | 3.39 | 1.17E-12 |
| hsa-miR-335-5p | MIRT017317 | LONRF2 | -2.61 | 1.05E-10 |
| hsa-miR-335-5p | MIRT017342 | COL10A1 | 5.83 | 1.17E-12 |
| hsa-miR-335-5p | MIRT017349 | DMBX1 | 3.86 | 8.42E-12 |
| hsa-miR-335-5p | MIRT017350 | PPP1R3C | -2.95 | 1.49E-19 |
| hsa-miR-335-5p | MIRT017371 | PLIN4 | -3.82 | 1.19E-19 |
| hsa-miR-335-5p | MIRT017377 | TMEFF2 | -2.55 | 2.33E-11 |
| hsa-miR-335-5p | MIRT017386 | SCG3 | -2.67 | 9.76E-10 |
| hsa-miR-335-5p | MIRT017395 | CLDN4 | 2.52 | 1.32E-10 |
| hsa-miR-335-5p | MIRT017398 | R3HDML | 2.55 | 3.71E-12 |
| hsa-miR-335-5p | MIRT017399 | ABCA8 | -2.99 | 4.54E-16 |
| hsa-miR-335-5p | MIRT017405 | SULT2A1 | -3.00 | 1.45E-07 |
| hsa-miR-335-5p | MIRT017414 | COL11A1 | 4.94 | 1.34E-09 |
| hsa-miR-335-5p | MIRT017431 | CELSR3 | 2.20 | 2.30E-10 |
| hsa-miR-335-5p | MIRT017434 | XKR4 | -3.14 | 6.35E-18 |
| hsa-miR-335-5p | MIRT017438 | UBD | 2.83 | 8.46E-08 |
| hsa-miR-335-5p | MIRT017445 | SNCG | -2.21 | 1.89E-14 |
| hsa-miR-335-5p | MIRT017448 | MUC3A | 2.41 | 1.15E-04 |
| hsa-miR-335-5p | MIRT017451 | CDH3 | 2.77 | 2.64E-10 |
| hsa-miR-335-5p | MIRT017452 | GPIHBP1 | -2.06 | 1.17E-12 |
| hsa-miR-335-5p | MIRT017453 | HTRA4 | 2.92 | 7.96E-16 |
| hsa-miR-335-5p | MIRT017464 | LY6H | -2.39 | 1.60E-13 |
| hsa-miR-335-5p | MIRT017510 | CLDN1 | 3.08 | 1.17E-12 |
| hsa-miR-335-5p | MIRT017511 | ENTPD3 | -2.51 | 1.17E-12 |
| hsa-miR-335-5p | MIRT017526 | SMYD1 | -3.17 | 1.74E-06 |
| hsa-miR-335-5p | MIRT017560 | CHRM2 | -3.47 | 8.25E-10 |
| hsa-miR-335-5p | MIRT017565 | RSPO1 | -2.41 | 2.68E-10 |
| hsa-miR-335-5p | MIRT017577 | CST4 | 3.72 | 4.03E-22 |
| hsa-miR-335-5p | MIRT017599 | RPS6KA6 | -2.96 | 3.42E-17 |
| hsa-miR-335-5p | MIRT017610 | 4 | -2.82 | 2.13E-09 |
| hsa-miR-335-5p | MIRT017613 | TERT | 2.36 | 9.14E-07 |
| hsa-miR-335-5p | MIRT017615 | SLC17A7 | -2.02 | 4.33E-13 |

© 2021 Izumi D et al. *JAMA Network Open.*

| | | | | |
|---|---|---|---|---|
| hsa-miR-335-5p | MIRT017622 | FOXD3 | -2.91 | 1.30E-12 |
| hsa-miR-335-5p | MIRT017688 | CCL14 | -2.09 | 4.33E-12 |
| hsa-miR-335-5p | MIRT017697 | FNDC1 | 3.08 | 7.87E-08 |
| hsa-miR-335-5p | MIRT017702 | C6orf58 | -3.03 | 1.92E-07 |
| hsa-miR-335-5p | MIRT017703 | LRAT | -2.80 | 1.54E-10 |
| hsa-miR-335-5p | MIRT017705 | LAIR2 | 2.01 | 6.12E-06 |
| hsa-miR-335-5p | MIRT017706 | GUCA2B | -2.87 | 1.39E-08 |
| hsa-miR-335-5p | MIRT017708 | PRKCG | 2.55 | 7.16E-06 |
| hsa-miR-335-5p | MIRT017731 | CLEC3B | -3.69 | 3.17E-49 |
| hsa-miR-335-5p | MIRT017735 | KIT | -2.18 | 3.91E-15 |
| hsa-miR-335-5p | MIRT017751 | BVES-AS1 | -2.70 | 2.90E-13 |
| hsa-miR-335-5p | MIRT017769 | TSLP | -2.45 | 2.13E-17 |
| hsa-miR-335-5p | MIRT017782 | MISP | 2.73 | 5.58E-12 |
| hsa-miR-335-5p | MIRT017841 | TACR2 | -2.96 | 4.57E-11 |
| hsa-miR-335-5p | MIRT017846 | TREH | -2.17 | 2.45E-11 |
| hsa-miR-335-5p | MIRT017858 | SOX9 | 2.59 | 3.03E-19 |
| hsa-miR-335-5p | MIRT017862 | LIPG | 2.10 | 1.55E-09 |
| hsa-miR-335-5p | MIRT017878 | CLDN7 | 2.21 | 3.47E-12 |
| hsa-miR-335-5p | MIRT017902 | ENDOU | -2.79 | 5.65E-14 |
| hsa-miR-335-5p | MIRT017921 | SORCS3 | -2.78 | 3.25E-12 |
| hsa-miR-335-5p | MIRT017927 | PNLIPRP3 | -2.61 | 5.36E-08 |
| hsa-miR-335-5p | MIRT017934 | PEBP4 | -3.66 | 7.13E-27 |
| hsa-miR-335-5p | MIRT017935 | GSG1L | -2.27 | 4.09E-14 |
| hsa-miR-335-5p | MIRT017936 | WDR17 | -2.26 | 2.37E-10 |
| hsa-miR-335-5p | MIRT017953 | PABPC1L | 2.21 | 1.51E-12 |
| hsa-miR-335-5p | MIRT017984 | XIRP1 | 2.57 | 9.35E-08 |
| hsa-miR-335-5p | MIRT017988 | SMOC2 | -2.04 | 1.80E-09 |
| hsa-miR-335-5p | MIRT018001 | CTHRC1 | 3.10 | 8.77E-15 |
| hsa-miR-335-5p | MIRT018039 | SOSTDC1 | -4.41 | 1.61E-23 |
| hsa-miR-335-5p | MIRT018041 | TRIM50 | -3.10 | 1.90E-12 |
| hsa-miR-335-5p | MIRT018048 | LGALS9C | -2.70 | 9.96E-12 |
| hsa-miR-335-5p | MIRT018057 | LIF | 2.14 | 2.44E-12 |
| hsa-miR-335-5p | MIRT018066 | MAL2 | 2.19 | 1.43E-12 |
| hsa-miR-335-5p | MIRT018068 | GSN | -2.06 | 1.62E-30 |
| hsa-miR-335-5p | MIRT018085 | ATP6V0D2 | 2.39 | 1.89E-08 |
| hsa-miR-335-5p | MIRT018126 | LMOD1 | -3.28 | 1.48E-18 |
| hsa-miR-335-5p | MIRT018192 | NOVA1 | -2.36 | 1.17E-12 |
| hsa-miR-335-5p | MIRT018205 | ANK2 | -2.12 | 2.99E-11 |
| hsa-miR-335-5p | MIRT018209 | CRNN | -2.84 | 4.39E-04 |
| hsa-miR-335-5p | MIRT018220 | CCDC69 | -2.36 | 1.03E-22 |
| hsa-miR-335-5p | MIRT018249 | ADAMTS12 | 2.90 | 5.65E-14 |
| hsa-miR-335-5p | MIRT018277 | CST1 | 6.74 | 1.17E-12 |
| hsa-miR-335-5p | MIRT018278 | CXCL3 | 2.13 | 7.27E-06 |
| hsa-miR-335-5p | MIRT018281 | PDZD4 | -2.78 | 2.10E-17 |
| hsa-miR-335-5p | MIRT018310 | PPP1R1A | -4.21 | 1.12E-23 |

© 2021 Izumi D et al. *JAMA Network Open.*

| | | | | |
|---|---|---|---|---|
| hsa-miR-335-5p | MIRT018332 | BCHE | -3.24 | 3.41E-17 |
| hsa-miR-335-5p | MIRT018333 | GIP | -3.53 | 1.46E-12 |
| hsa-miR-335-5p | MIRT018336 | HS6ST3 | -3.15 | 2.90E-13 |
| hsa-miR-335-5p | MIRT018338 | APOC1 | 3.10 | 1.09E-12 |
| hsa-miR-335-5p | MIRT018340 | HAVCR1 | 2.30 | 4.13E-04 |
| hsa-miR-335-5p | MIRT018353 | NPY1R | -2.13 | 2.96E-07 |
| hsa-miR-335-5p | MIRT018375 | PKD2L1 | 2.81 | 1.21E-16 |
| hsa-miR-335-5p | MIRT018397 | BEX2 | -2.51 | 2.93E-08 |
| hsa-miR-335-5p | MIRT018430 | ASCL2 | 2.29 | 1.06E-04 |
| hsa-miR-335-5p | MIRT018431 | SNAP91 | -2.32 | 3.25E-07 |
| hsa-miR-335-5p | MIRT018443 | RASGEF1C | -2.26 | 3.47E-11 |
| hsa-miR-335-5p | MIRT018447 | ABCC8 | -2.30 | 5.58E-09 |
| hsa-miR-335-5p | MIRT018455 | FOXD2 | 2.32 | 2.44E-13 |
| hsa-miR-335-5p | MIRT018459 | BAAT | 3.94 | 2.78E-08 |
| hsa-miR-335-5p | MIRT018464 | MLN | -2.23 | 3.70E-05 |
| hsa-miR-335-5p | MIRT018484 | CHST9 | -3.07 | 2.25E-09 |
| hsa-miR-335-5p | MIRT018515 | CDH19 | -3.91 | 7.16E-18 |
| hsa-miR-335-5p | MIRT018520 | DEFB4A | -2.47 | 1.84E-05 |
| hsa-miR-335-5p | MIRT018522 | GJB4 | 2.46 | 2.89E-05 |
| hsa-miR-335-5p | MIRT018542 | ZBTB7C | -2.24 | 2.28E-09 |
| hsa-miR-335-5p | MIRT018544 | FGF10 | -2.03 | 4.82E-07 |
| hsa-miR-335-5p | MIRT018574 | GATA5 | -2.03 | 1.55E-03 |
| hsa-miR-335-5p | MIRT018587 | CHL1 | -2.14 | 4.19E-12 |
| hsa-miR-335-5p | MIRT018593 | SCARA5 | -4.54 | 3.45E-35 |
| hsa-miR-335-5p | MIRT018598 | NT5C1A | -3.11 | 8.57E-23 |
| hsa-miR-335-5p | MIRT018642 | GCNT4 | -2.93 | 3.73E-22 |
| hsa-miR-335-5p | MIRT018670 | CDX2 | 3.11 | 2.78E-05 |
| hsa-miR-335-5p | MIRT018703 | GDF15 | 3.13 | 3.48E-13 |
| hsa-miR-335-5p | MIRT018735 | CGNL1 | -2.12 | 3.40E-13 |
| hsa-miR-335-5p | MIRT018740 | ADH7 | -6.35 | 4.69E-32 |
| hsa-miR-335-5p | MIRT018757 | TPO | -2.09 | 8.20E-08 |
| hsa-miR-335-5p | MIRT018762 | LGALS9B | -2.78 | 1.38E-11 |
| hsa-miR-335-5p | MIRT018772 | COL4A5 | -2.42 | 2.89E-13 |
| hsa-miR-335-5p | MIRT018779 | CNTD2 | 2.23 | 8.93E-06 |
| hsa-miR-335-5p | MIRT018781 | FGL2 | -2.13 | 3.18E-13 |
| hsa-miR-335-5p | MIRT018787 | PEG3 | -2.12 | 1.09E-11 |
| hsa-miR-335-5p | MIRT018793 | ADGRB3 | -2.61 | 1.21E-12 |
| hsa-miR-335-5p | MIRT018814 | HPDL | 2.06 | 1.01E-07 |
| hsa-miR-335-5p | MIRT018815 | ASB2 | -2.66 | 1.09E-15 |
| hsa-miR-335-5p | MIRT018818 | CST2 | 3.06 | 3.37E-08 |
| hsa-miR-335-5p | MIRT018820 | ADGRG4 | -3.48 | 4.54E-17 |
| hsa-miR-335-5p | MIRT018828 | AQP10 | -3.63 | 7.75E-16 |
| hsa-miR-335-5p | MIRT018837 | EMILIN3 | -2.83 | 1.12E-25 |
| hsa-miR-335-5p | MIRT018862 | SLC6A4 | -2.76 | 2.22E-17 |
| hsa-miR-335-5p | MIRT018894 | ENHO | -2.19 | 9.38E-10 |

© 2021 Izumi D et al. *JAMA Network Open.*

| | | | | |
|---|---|---|---|---|
| hsa-miR-335-5p | MIRT018900 | DCSTAMP | 3.05 | 6.17E-14 |
| hsa-miR-335-5p | MIRT018910 | PDK4 | -3.08 | 2.84E-21 |
| hsa-miR-335-5p | MIRT018916 | CPE | -2.15 | 7.07E-15 |
| hsa-miR-335-5p | MIRT018933 | CD36 | -2.13 | 2.05E-16 |
| hsa-miR-335-5p | MIRT018952 | CALML5 | -2.09 | 3.14E-04 |
| hsa-miR-335-5p | MIRT018965 | RSPO2 | -3.59 | 1.90E-19 |
| hsa-miR-335-5p | MIRT018980 | PCSK9 | 2.11 | 8.38E-05 |
| hsa-miR-335-5p | MIRT018981 | VEGFD | -4.15 | 9.22E-41 |
| hsa-miR-335-5p | MIRT018996 | GNGT1 | 2.28 | 6.00E-04 |
| hsa-miR-335-5p | MIRT019004 | FHL1 | -3.31 | 1.26E-25 |
| hsa-miR-335-5p | MIRT019012 | CPO | -2.31 | 2.55E-13 |
| hsa-miR-335-5p | MIRT019032 | CXCL8 | 2.72 | 1.46E-06 |
| hsa-miR-335-5p | MIRT019040 | FABP4 | -3.47 | 1.13E-20 |
| hsa-miR-335-5p | MIRT019060 | HMGCLL1 | -2.78 | 3.35E-16 |
| hsa-miR-335-5p | MIRT019062 | SFTPD | -2.14 | 2.07E-08 |
| hsa-miR-335-5p | MIRT019069 | ANKS4B | 2.11 | 3.66E-05 |
| hsa-miR-335-5p | MIRT019084 | GPER1 | -2.62 | 9.25E-18 |
| hsa-miR-335-5p | MIRT019097 | DIRAS1 | -2.74 | 1.17E-14 |
| hsa-miR-335-5p | MIRT019104 | SPINK7 | -3.88 | 3.56E-13 |
| hsa-miR-335-5p | MIRT019110 | ATP1B2 | -2.02 | 4.21E-14 |
| hsa-miR-335-5p | MIRT019111 | SLC2A4 | -3.08 | 4.25E-21 |
| hsa-miR-335-5p | MIRT019119 | FAM189A1 | -2.56 | 2.36E-08 |
| hsa-miR-335-5p | MIRT019120 | RERGL | -2.90 | 5.10E-15 |
| hsa-miR-335-5p | MIRT019174 | TMEM132C | -3.85 | 7.31E-22 |
| hsa-miR-335-5p | MIRT019185 | GDF10 | -2.73 | 1.48E-10 |
| hsa-miR-335-5p | MIRT019192 | MSLN | 2.87 | 1.52E-04 |
| hsa-miR-335-5p | MIRT019202 | PKHD1L1 | -2.68 | 2.19E-17 |
| hsa-miR-335-5p | MIRT019216 | ASTN1 | -2.48 | 4.40E-08 |
| hsa-miR-335-5p | MIRT019223 | HTR1D | 2.08 | 8.29E-04 |
| hsa-miR-335-5p | MIRT019225 | MYOT | -2.80 | 8.21E-19 |
| hsa-miR-181a-5p | MIRT025043 | FXYD6 | -2.16 | 1.70E-14 |
| hsa-miR-181a-5p | MIRT025054 | PHOX2A | -2.66 | 2.99E-10 |
| hsa-miR-181a-5p | MIRT025057 | GSTM2 | -2.06 | 7.77E-24 |
| hsa-miR-181a-5p | MIRT025060 | PTPRZ1 | -2.65 | 5.37E-10 |
| hsa-miR-181a-5p | MIRT025069 | NMRK2 | -2.32 | 1.75E-10 |
| hsa-miR-181a-5p | MIRT025070 | WNT2 | 4.09 | 5.04E-13 |
| hsa-miR-181a-5p | MIRT025134 | OFCC1 | 2.14 | 9.78E-12 |
| hsa-miR-181a-5p | MIRT025148 | CHL1 | -2.14 | 4.19E-12 |
| hsa-miR-181a-5p | MIRT025163 | PCLAF | 2.23 | 3.45E-15 |
| hsa-miR-196a-5p | MIRT026059 | IGF2BP3 | 3.23 | 2.17E-07 |
| hsa-miR-196a-5p | MIRT026082 | PRUNE2 | -2.51 | 6.39E-10 |
| hsa-miR-196a-5p | MIRT026092 | EPHA7 | -2.82 | 3.83E-10 |
| hsa-miR-196a-5p | MIRT026098 | IGF2BP1 | 3.25 | 1.36E-04 |
| hsa-miR-93-5p | MIRT027944 | TMEM100 | -3.70 | 6.42E-26 |
| hsa-miR-93-5p | MIRT027950 | ZIC5 | 3.10 | 1.60E-04 |

© 2021 Izumi D et al. *JAMA Network Open.*

| | | | | |
|---|---|---|---|---|
| hsa-miR-93-5p | MIRT027969 | FAM129A | -2.16 | 2.35E-14 |
| hsa-miR-93-5p | MIRT028167 | PRUNE2 | -2.51 | 6.39E-10 |
| hsa-miR-93-5p | MIRT028172 | EPHA7 | -2.82 | 3.83E-10 |
| hsa-miR-21-5p | MIRT030694 | SOX2 | -2.30 | 1.88E-05 |
| hsa-miR-21-5p | MIRT030776 | LONRF2 | -2.61 | 1.05E-10 |
| hsa-miR-21-5p | MIRT030815 | KNL1 | 2.19 | 5.78E-16 |
| hsa-miR-21-5p | MIRT030819 | FAXDC2 | -2.26 | 5.40E-20 |
| hsa-miR-21-5p | MIRT030871 | MMP9 | 2.32 | 2.89E-08 |
| hsa-miR-21-5p | MIRT030888 | DMD | -2.05 | 2.08E-12 |
| hsa-miR-21-5p | MIRT030914 | TOP2A | 2.79 | 3.08E-16 |
| hsa-miR-21-5p | MIRT030986 | HOXA9 | 2.85 | 2.84E-07 |
| hsa-miR-21-5p | MIRT031012 | OLR1 | 2.89 | 5.14E-12 |
| hsa-miR-21-5p | MIRT031067 | TNFRSF11B | 2.07 | 1.16E-05 |
| hsa-miR-18a-5p | MIRT031333 | HOXA9 | 2.85 | 2.84E-07 |
| hsa-miR-93-3p | MIRT038720 | HASPIN | 2.26 | 1.26E-16 |
| hsa-miR-93-3p | MIRT038725 | CSAG1 | 2.94 | 6.76E-04 |
| hsa-miR-93-3p | MIRT038774 | CENPF | 2.76 | 2.92E-19 |
| hsa-miR-93-3p | MIRT038799 | HMMR | 2.57 | 2.53E-18 |
| hsa-miR-93-3p | MIRT038870 | CDC20 | 2.20 | 1.17E-12 |
| hsa-miR-18a-3p | MIRT040758 | GINS1 | 2.11 | 2.01E-16 |
| hsa-miR-18a-3p | MIRT040765 | C6orf222 | 2.75 | 5.26E-07 |
| hsa-miR-18a-3p | MIRT040818 | CACNA2D3 | -2.03 | 1.02E-13 |
| hsa-miR-18a-3p | MIRT040857 | CDCA2 | 2.69 | 3.41E-17 |
| hsa-miR-18a-3p | MIRT040875 | PTGS1 | -2.10 | 8.56E-22 |
| hsa-miR-18a-3p | MIRT040934 | ASF1B | 2.07 | 3.05E-14 |
| hsa-miR-18a-3p | MIRT040971 | CLU | -2.04 | 3.41E-10 |
| hsa-miR-196b-5p | MIRT042665 | SLC6A15 | -2.53 | 7.84E-08 |
| hsa-miR-196b-5p | MIRT042672 | HTR1D | 2.08 | 8.29E-04 |
| hsa-miR-196b-5p | MIRT042674 | CKB | -2.89 | 1.99E-21 |
| hsa-miR-196b-5p | MIRT042691 | BUB1 | 2.67 | 4.33E-20 |
| hsa-miR-196a-5p | MIRT048156 | NRXN1 | -3.79 | 9.40E-22 |
| hsa-miR-196a-5p | MIRT048176 | REEP2 | -2.08 | 2.54E-11 |
| hsa-miR-196a-5p | MIRT048197 | UBE2C | 2.82 | 1.78E-15 |
| hsa-miR-196a-5p | MIRT048215 | CKAP2L | 2.25 | 7.43E-18 |
| hsa-miR-196a-5p | MIRT048234 | KIF18B | 3.06 | 1.88E-21 |
| hsa-miR-196a-5p | MIRT048236 | SH3GL3 | -2.21 | 2.39E-07 |
| hsa-miR-196a-5p | MIRT048279 | BUB1 | 2.67 | 4.33E-20 |
| hsa-miR-93-5p | MIRT048739 | ZIC2 | 2.89 | 4.99E-04 |
| hsa-miR-93-5p | MIRT048806 | BIRC5 | 2.24 | 3.78E-13 |
| hsa-miR-18a-5p | MIRT050708 | CDC20 | 2.20 | 1.17E-12 |
| hsa-miR-18a-5p | MIRT050725 | PKMYT1 | 2.62 | 1.86E-16 |
| hsa-miR-18a-5p | MIRT050732 | CDCA5 | 2.33 | 7.22E-16 |
| hsa-miR-181a-5p | MIRT052993 | PGR | -2.11 | 1.37E-12 |
| hsa-miR-93-5p | MIRT053085 | SLC2A4 | -3.08 | 4.25E-21 |
| hsa-miR-21-5p | MIRT053173 | HPGD | -2.95 | 1.79E-19 |

© 2021 Izumi D et al. *JAMA Network Open.*

| | | | | |
|---|---|---|---|---|
| hsa-miR-196b-5p | MIRT053330 | HOXA9 | 2.85 | 2.84E-07 |
| hsa-miR-146b-5p | MIRT053567 | UHRF1 | 2.30 | 1.58E-16 |
| hsa-miR-196b-5p | MIRT053586 | HOXA10 | 4.24 | 2.35E-09 |
| hsa-miR-181a-5p | MIRT053664 | TNFRSF11B | 2.07 | 1.16E-05 |
| hsa-miR-181a-5p | MIRT053680 | BMP3 | -2.98 | 4.96E-08 |
| hsa-miR-181a-5p | MIRT053690 | ACAN | 3.62 | 2.65E-18 |
| hsa-miR-196b-5p | MIRT066479 | HMGA2 | 2.93 | 3.84E-07 |
| hsa-miR-93-5p | MIRT084345 | RRM2 | 2.29 | 2.20E-14 |
| hsa-miR-181b-3p | MIRT118893 | LONRF2 | -2.61 | 1.05E-10 |
| hsa-miR-181a-5p | MIRT138427 | KIF2C | 2.05 | 1.34E-14 |
| hsa-miR-181b-5p | MIRT138428 | KIF2C | 2.05 | 1.34E-14 |
| hsa-miR-18a-5p | MIRT273157 | RAD51AP1 | 2.11 | 8.77E-18 |
| hsa-miR-18a-5p | MIRT282668 | SYNM | -3.39 | 2.93E-15 |
| hsa-miR-135b-5p | MIRT289438 | BIRC5 | 2.24 | 3.78E-13 |
| hsa-miR-146b-5p | MIRT437621 | S100A12 | -2.45 | 4.90E-10 |
| hsa-miR-93-5p | MIRT437750 | SLC16A9 | -2.24 | 4.05E-09 |
| hsa-miR-181a-5p | MIRT437924 | TERT | 2.36 | 9.14E-07 |
| hsa-miR-181a-5p | MIRT437969 | IFNG | 2.00 | 1.96E-05 |
| hsa-miR-93-5p | MIRT438087 | CXCL8 | 2.72 | 1.46E-06 |
| hsa-miR-21-5p | MIRT438112 | CXCL10 | 2.14 | 9.57E-06 |
| hsa-miR-21-5p | MIRT438224 | CLU | -2.04 | 3.41E-10 |
| hsa-miR-181a-5p | MIRT438437 | WIF1 | -3.90 | 1.76E-15 |
| hsa-miR-18a-5p | MIRT442747 | PTCHD1 | -3.31 | 3.35E-15 |
| hsa-miR-196b-3p | MIRT443008 | KBTBD12 | -2.09 | 8.79E-06 |
| hsa-miR-146b-5p | MIRT448042 | SFRP1 | -4.23 | 2.09E-25 |
| hsa-miR-135b-5p | MIRT448598 | PCP4L1 | -3.59 | 1.94E-15 |
| hsa-miR-335-3p | MIRT449054 | MGAT4C | -2.06 | 2.73E-07 |
| hsa-miR-146b-5p | MIRT449334 | ACTBL2 | 2.34 | 1.62E-07 |
| hsa-miR-135b-5p | MIRT449577 | APOA1 | -2.69 | 2.71E-05 |
| hsa-miR-93-5p | MIRT450918 | CADM2 | -3.87 | 5.33E-21 |
| hsa-miR-18a-3p | MIRT467476 | SMYD1 | -3.17 | 1.74E-06 |
| hsa-miR-93-5p | MIRT494434 | BTG2 | -2.01 | 4.03E-23 |
| hsa-miR-93-5p | MIRT506852 | KIF23 | 2.43 | 2.05E-20 |
| hsa-miR-93-5p | MIRT506883 | PCLAF | 2.23 | 3.45E-15 |
| hsa-miR-196a-5p | MIRT507497 | E2F7 | 2.67 | 2.28E-16 |
| hsa-miR-196b-5p | MIRT507498 | E2F7 | 2.67 | 2.28E-16 |
| hsa-miR-181b-3p | MIRT513264 | SCUBE1 | -2.44 | 3.81E-16 |
| hsa-miR-93-5p | MIRT513708 | RBM20 | -2.31 | 1.25E-12 |
| hsa-miR-93-5p | MIRT517183 | SLC28A1 | -2.41 | 1.36E-09 |
| hsa-miR-93-5p | MIRT518695 | KCNMB1 | -2.79 | 6.47E-18 |
| hsa-miR-146b-3p | MIRT526287 | KY | -2.08 | 1.06E-11 |
| hsa-miR-18a-3p | MIRT526291 | KY | -2.08 | 1.06E-11 |
| hsa-miR-93-3p | MIRT528115 | FOXH1 | 2.68 | 4.51E-08 |
| hsa-miR-181b-3p | MIRT529502 | IYD | 2.57 | 2.42E-05 |
| hsa-miR-135b-3p | MIRT531366 | SPC25 | 2.03 | 6.73E-15 |

© 2021 Izumi D et al. *JAMA Network Open.*

| | | | | |
|---|---|---|---|---|
| hsa-miR-181a-5p | MIRT535284 | PHOX2B | -2.72 | 4.83E-10 |
| hsa-miR-181b-5p | MIRT535285 | PHOX2B | -2.72 | 4.83E-10 |
| hsa-miR-335-5p | MIRT536189 | MAOB | -2.47 | 4.00E-14 |
| hsa-miR-196a-3p | MIRT540504 | CXCL10 | 2.14 | 9.57E-06 |
| hsa-miR-196b-5p | MIRT547839 | IGF2BP3 | 3.23 | 2.17E-07 |
| hsa-miR-196a-5p | MIRT547902 | HOXA9 | 2.85 | 2.84E-07 |
| hsa-miR-135b-5p | MIRT549355 | ARC | -3.13 | 4.14E-15 |
| hsa-miR-196b-5p | MIRT555194 | PRUNE2 | -2.51 | 6.39E-10 |
| hsa-miR-181b-5p | MIRT557275 | HMGA2 | 2.93 | 3.84E-07 |
| hsa-miR-181a-5p | MIRT557276 | HMGA2 | 2.93 | 3.84E-07 |
| hsa-miR-335-3p | MIRT562743 | AOC3 | -2.15 | 1.10E-12 |
| hsa-miR-93-5p | MIRT567057 | KCNB1 | -3.66 | 1.81E-18 |
| hsa-miR-335-3p | MIRT569802 | XKR4 | -3.14 | 6.35E-18 |
| hsa-miR-146b-5p | MIRT609587 | GPM6B | -2.47 | 9.20E-26 |
| hsa-miR-335-3p | MIRT609698 | GFRA1 | -3.38 | 4.44E-17 |
| hsa-miR-335-3p | MIRT610269 | PCSK2 | -4.53 | 9.59E-27 |
| hsa-miR-335-3p | MIRT615437 | FAXC | -2.09 | 9.72E-08 |
| hsa-miR-93-5p | MIRT615447 | FAXC | -2.09 | 9.72E-08 |
| hsa-miR-335-3p | MIRT616818 | FGF10 | -2.03 | 4.82E-07 |
| hsa-miR-335-3p | MIRT618054 | PCDH19 | -2.15 | 1.17E-12 |
| hsa-miR-335-3p | MIRT623191 | MYOCD | -2.69 | 1.16E-13 |
| hsa-miR-196a-3p | MIRT627264 | XKR4 | -3.14 | 6.35E-18 |
| hsa-miR-93-5p | MIRT628565 | MELK | 2.59 | 2.19E-18 |
| hsa-miR-181b-5p | MIRT633492 | WDR72 | 3.49 | 1.46E-05 |
| hsa-miR-181a-5p | MIRT633493 | WDR72 | 3.49 | 1.46E-05 |
| hsa-miR-18a-3p | MIRT638250 | SLC16A9 | -2.24 | 4.05E-09 |
| hsa-miR-335-3p | MIRT638317 | RNF150 | -2.17 | 1.88E-10 |
| hsa-miR-18a-3p | MIRT638737 | FAXC | -2.09 | 9.72E-08 |
| hsa-miR-335-3p | MIRT639081 | ADCYAP1 | -2.03 | 2.37E-06 |
| hsa-miR-181b-3p | MIRT642414 | CILP2 | 2.57 | 2.55E-07 |
| hsa-miR-335-3p | MIRT642579 | PCLAF | 2.23 | 3.45E-15 |
| hsa-miR-335-3p | MIRT650016 | ADAMTS8 | -2.04 | 1.81E-07 |
| hsa-miR-93-5p | MIRT685721 | BHMT2 | -2.30 | 1.31E-14 |
| hsa-miR-93-5p | MIRT694951 | ANKS4B | 2.11 | 3.66E-05 |
| hsa-miR-93-5p | MIRT699286 | SLC6A4 | -2.76 | 2.22E-17 |
| hsa-miR-146b-3p | MIRT704958 | CBX2 | 2.17 | 2.10E-08 |
| hsa-miR-196a-3p | MIRT708479 | OLR1 | 2.89 | 5.14E-12 |
| hsa-miR-335-3p | MIRT708630 | STMN4 | -2.02 | 2.87E-08 |
| hsa-miR-18a-3p | MIRT709746 | UBD | 2.83 | 8.46E-08 |
| hsa-miR-93-3p | MIRT709918 | GRIK3 | -3.64 | 2.69E-20 |
| hsa-miR-146b-3p | MIRT710266 | FAM107A | -2.91 | 9.59E-27 |
| hsa-miR-18a-3p | MIRT710270 | FAM107A | -2.91 | 9.59E-27 |
| hsa-miR-196a-3p | MIRT711377 | SKA1 | 2.16 | 1.59E-14 |
| hsa-miR-18a-3p | MIRT711961 | CYP27B1 | 2.17 | 1.17E-12 |
| hsa-miR-93-3p | MIRT716717 | SCN7A | -3.84 | 3.41E-19 |

© 2021 Izumi D et al. *JAMA Network Open.*

| | | | | |
|---|---|---|---|---|
| hsa-miR-93-3p | MIRT717236 | SH2D5 | 2.04 | 7.45E-06 |
| hsa-miR-146b-3p | MIRT717691 | PTGS1 | -2.10 | 8.56E-22 |
| hsa-miR-146b-5p | MIRT717743 | MYLK | -2.18 | 4.63E-11 |
| hsa-miR-335-3p | MIRT718902 | GALR1 | -2.56 | 9.03E-12 |
| hsa-miR-335-3p | MIRT722849 | NEGR1 | -2.56 | 6.06E-17 |
| hsa-miR-93-5p | MIRT726903 | POLQ | 2.55 | 4.16E-17 |
| hsa-miR-93-5p | MIRT726927 | PKMYT1 | 2.62 | 1.86E-16 |
| hsa-miR-181b-5p | MIRT727098 | NCAPG | 2.38 | 3.79E-16 |
| hsa-miR-181a-5p | MIRT727100 | NCAPG | 2.38 | 3.79E-16 |
| hsa-miR-181b-5p | MIRT732307 | SPP1 | 3.09 | 1.75E-07 |
| hsa-miR-18a-5p | MIRT732587 | MYLK | -2.18 | 4.63E-11 |
| hsa-miR-181b-5p | MIRT732607 | TNFRSF11B | 2.07 | 1.16E-05 |
| hsa-miR-181b-5p | MIRT732608 | TNFSF11 | 2.76 | 5.71E-14 |
| hsa-miR-135b-5p | MIRT732742 | ADAM12 | 3.21 | 4.85E-13 |
| hsa-miR-196a-5p | MIRT732869 | HOXA10 | 4.24 | 2.35E-09 |
| hsa-miR-146b-5p | MIRT732960 | NOVA1 | -2.36 | 1.17E-12 |
| hsa-miR-196a-5p | MIRT733362 | MAMDC2 | -4.28 | 8.61E-32 |
| hsa-miR-21-3p | MIRT733453 | HPGD | -2.95 | 1.79E-19 |
| hsa-miR-135b-3p | MIRT733901 | CCL7 | 2.70 | 1.84E-11 |
| hsa-miR-21-5p | MIRT734186 | MSLN | 2.87 | 1.52E-04 |
| hsa-miR-181a-5p | MIRT734362 | PRKN | -2.13 | 1.60E-20 |
| hsa-miR-196b-5p | MIRT734448 | IGF2BP1 | 3.25 | 1.36E-04 |
| hsa-miR-93-3p | MIRT734847 | MMP3 | 3.45 | 1.53E-05 |
| hsa-miR-135b-5p | MIRT734929 | THBS2 | 2.10 | 1.68E-06 |
| hsa-miR-146b-3p | MIRT734967 | NPAS4 | -2.53 | 1.10E-12 |
| hsa-miR-146b-5p | MIRT735151 | SLC5A5 | -3.32 | 3.58E-10 |
| hsa-miR-93-5p | MIRT735341 | MMP3 | 3.45 | 1.53E-05 |
| hsa-miR-181b-3p | MIRT738031 | RBM20 | -2.31 | 1.25E-12 |
| hsa-miR-18a-3p | MIRT738296 | SH2D5 | 2.04 | 7.45E-06 |
| hsa-miR-335-3p | MIRT741342 | HMGA2 | 2.93 | 3.84E-07 |
| hsa-miR-93-3p | MIRT760677 | CXCL5 | 2.39 | 9.01E-03 |
| hsa-miR-18a-3p | MIRT763227 | EPHA6 | -2.86 | 2.30E-11 |
| hsa-miR-196a-3p | MIRT763520 | WT1 | 2.19 | 2.71E-04 |
| hsa-miR-335-3p | MIRT765641 | MAGEA12 | 3.37 | 3.86E-07 |
| hsa-miR-21-3p | MIRT790183 | RGS2 | -2.06 | 2.04E-19 |

© 2021 Izumi D et al. *JAMA Network Open.*

**eTable 3.** Functional analysis of miRNA target genes identified 61 significantly enriched functional gene sets (BH-adjusted p-value < 0.0001)

| Gene Set | Gene Ratio | *P* value | BH-adjusted *P* value |
|---|---|---|---|
| VECCHI GASTRIC CANCER EARLY DN | 39/317 | 3.07E-22 | 1.99E-18 |
| VECCHI GASTRIC CANCER EARLY UP | 39/317 | 4.81E-20 | 1.56E-16 |
| BOQUEST STEM CELL CULTURED VS FRESH UP | 34/317 | 5.43E-16 | 8.81E-13 |
| SABATES COLORECTAL ADENOMA DN | 29/317 | 4.15E-16 | 8.81E-13 |
| NABA SECRETED FACTORS | 25/317 | 3.21E-11 | 1.90E-08 |
| SMID BREAST CANCER NORMAL LIKE UP | 24/317 | 1.40E-07 | 2.21E-05 |
| POOLA INVASIVE BREAST CANCER UP | 23/317 | 4.30E-11 | 2.32E-08 |
| MIKKELSEN NPC HCP WITH H3K27ME3 | 23/317 | 9.24E-10 | 3.16E-07 |
| RIGGI EWING SARCOMA PROGENITOR UP | 23/317 | 8.44E-08 | 1.52E-05 |
| GO SIGNAL RELEASE | 23/317 | 2.38E-07 | 3.36E-05 |
| HORIUCHI WTAP TARGETS DN | 22/317 | 1.20E-09 | 3.89E-07 |
| DUTERTRE ESTRADIOL RESPONSE 24HR UP | 22/317 | 1.81E-09 | 5.09E-07 |
| GO COLLAGEN CONTAINING EXTRACELLULAR MATRIX | 22/317 | 1.11E-07 | 1.84E-05 |
| GO EXTRACELLULAR STRUCTURE ORGANIZATION | 22/317 | 2.07E- | 3.05E-05 |

© 2021 Izumi D et al. *JAMA Network Open.*

| | | | |
|---|---|---|---|
| | | 07 | |
| ZHENG GLIOBLASTOMA PLASTICITY UP | 21/317 | 4.71E-11 | 2.35E-08 |
| GO G PROTEIN COUPLED RECEPTOR BINDING | 21/317 | 5.09E-10 | 1.94E-07 |
| FLORIO NEOCORTEX BASAL RADIAL GLIA DN | 20/317 | 4.35E-12 | 3.53E-09 |
| DELYS THYROID CANCER DN | 20/317 | 1.80E-10 | 7.79E-08 |
| AFFAR YY1 TARGETS DN | 20/317 | 7.74E-10 | 2.79E-07 |
| MEISSNER BRAIN HCP WITH H3K27ME3 | 20/317 | 1.52E-09 | 4.49E-07 |
| GO COGNITION | 20/317 | 9.69E-09 | 2.10E-06 |
| ROSTY CERVICAL CANCER PROLIFERATION CLUSTER | 19/317 | 1.51E-13 | 1.96E-10 |
| KOBAYASHI EGFR SIGNALING 24HR DN | 19/317 | 4.54E-09 | 1.13E-06 |
| DURAND STROMA S UP | 19/317 | 5.47E-08 | 1.07E-05 |
| SENGUPTA NASOPHARYNGEAL CARCINOMA UP | 19/317 | 7.93E-08 | 1.47E-05 |
| GO HORMONE TRANSPORT | 19/317 | 1.96E-07 | 2.96E-05 |
| YANG BCL3 TARGETS UP | 19/317 | 2.49E-07 | 3.36E-05 |
| CHIANG LIVER CANCER SUBCLASS PROLIFERATION UP | 18/317 | 1.12E-10 | 5.21E-08 |
| GO CYTOKINE ACTIVITY | 18/317 | 2.99E-09 | 8.04E-07 |

© 2021 Izumi D et al. *JAMA Network Open.*

| | | | |
|---|---|---|---|
| GO CYTOKINE RECEPTOR BINDING | 18/317 | 1.56E-07 | 2.41E-05 |
| LEE EARLY T LYMPHOCYTE UP | 17/317 | 2.87E-13 | 3.10E-10 |
| GRAHAM CML DIVIDING VS NORMAL QUIESCENT UP | 17/317 | 1.39E-09 | 4.30E-07 |
| GO REGULATION OF HORMONE SECRETION | 17/317 | 2.76E-07 | 3.58E-05 |
| NABA CORE MATRISOME | 17/317 | 5.18E-07 | 6.34E-05 |
| VECCHI GASTRIC CANCER ADVANCED VS EARLY UP | 16/317 | 4.98E-09 | 1.16E-06 |
| NAKAYAMA SOFT TISSUE TUMORS PCA2 UP | 15/317 | 2.28E-12 | 2.11E-09 |
| KONG E2F3 TARGETS | 15/317 | 7.15E-12 | 5.15E-09 |
| SOTIRIOU BREAST CANCER GRADE 1 VS 3 UP | 15/317 | 6.37E-09 | 1.43E-06 |
| GO MYELOID LEUKOCYTE MIGRATION | 15/317 | 2.55E-07 | 3.37E-05 |
| GO LEUKOCYTE CHEMOTAXIS | 15/317 | 6.74E-07 | 7.61E-05 |
| GO GLYCOSAMINOGLYCAN BINDING | 15/317 | 8.01E-07 | 8.81E-05 |
| ANDERSEN CHOLANGIOCARCINOMA CLASS2 | 14/317 | 2.44E-07 | 3.36E-05 |
| GRAHAM NORMAL QUIESCENT VS NORMAL DIVIDING DN | 13/317 | 4.38E-10 | 1.77E-07 |
| LE EGR2 TARGETS UP | 13/317 | 5.03E-09 | 1.16E-06 |

© 2021 Izumi D et al. *JAMA Network Open.*

| | | | |
|---|---|---|---|
| WILCOX RESPONSE TO PROGESTERONE UP | 13/317 | 3.29E-07 | 4.18E-05 |
| VART KSHV INFECTION ANGIOGENIC MARKERS UP | 13/317 | 6.35E-07 | 7.35E-05 |
| WINNEPENNINCKX MELANOMA METASTASIS UP | 13/317 | 6.35E-07 | 7.35E-05 |
| GO HEPARIN BINDING | 13/317 | 6.81E-07 | 7.61E-05 |
| KANG DOXORUBICIN RESISTANCE UP | 12/317 | 1.20E-11 | 7.78E-09 |
| NAKAYAMA SOFT TISSUE TUMORS PCA2 DN | 12/317 | 3.10E-09 | 8.04E-07 |
| TURASHVILI BREAST LOBULAR CARCINOMA VS LOBULAR NORMAL UP | 12/317 | 1.00E-08 | 2.10E-06 |
| WHITEFORD PEDIATRIC CANCER MARKERS | 12/317 | 1.09E-07 | 1.84E-05 |
| ZHOU CELL CYCLE GENES IN IR RESPONSE 24HR | 12/317 | 2.28E-07 | 3.29E-05 |
| GAVIN FOXP3 TARGETS CLUSTER P6 | 11/317 | 7.41E-08 | 1.41E-05 |
| CROONQUIST IL6 DEPRIVATION DN | 11/317 | 1.16E-07 | 1.88E-05 |
| GO CHEMOKINE RECEPTOR BINDING | 10/317 | 2.79E-08 | 5.65E-06 |
| RHODES UNDIFFERENTIATED CANCER | 9/317 | 5.99E-07 | 7.20E-05 |
| GO SOMATIC STEM CELL POPULATION MAINTENANCE | 9/317 | 8.67E-07 | 9.21E-05 |
| GO CHEMOKINE ACTIVITY | 8/317 | 3.69E-07 | 4.61E-05 |
| REICHERT MITOSIS LIN9 TARGETS | 7/317 | 1.05E- | 1.84E-05 |

© 2021 Izumi D et al. *JAMA Network Open.*

| | | | |
|---|---|---|---|
| | | 07 | |
| GO DOPAMINERGIC NEURON DIFFERENTIATION | 7/317 | 8.19E-07 | 8.85E-05 |

© 2021 Izumi D et al. *JAMA Network Open.*

**eTable 4.** Comparison between the expression of the 10 miRNAs in GC and normal frozen tissues

| **miRNA** | **AUC*** | **aveTumor**** | **aveNormal**** | **log2FC***** | ***P* value** |
|---|---|---|---|---|---|
| miR-21 | 0.72 | 5.58 | 4.62 | 0.96 | 7.3E-05 |
| miR-196a | 0.93 | -2.99 | -7.20 | 4.21 | 8.8E-14 |
| miR-146b | 0.59 | 1.19 | 0.61 | 0.58 | 5.4E-02 |
| miR-196b | 0.89 | -5.71 | -9.24 | 3.53 | 1.5E-11 |
| miR-135b | 0.40 | -5.59 | -4.84 | -0.75 | 9.6E-01 |
| miR-181b | 0.60 | -0.02 | -0.43 | 0.41 | 4.5E-02 |
| miR-181a | 0.58 | -1.61 | -2.00 | 0.39 | 7.5E-02 |
| miR-93 | 0.60 | 0.49 | 0.14 | 0.36 | 4.1E-02 |
| miR-335 | 0.62 | -4.05 | -4.44 | 0.38 | 1.7E-02 |
| miR-18a | 0.77 | -2.15 | -3.36 | 1.22 | 1.3E-06 |
| *AUC, area under the ROC curve. **ave, average. ***FC, fold change | | | | | |

© 2021 Izumi D et al. *JAMA Network Open.*

**eTable 5.** Statistical evaluation of the diagnostic value of the miRNAs in differentiating GC patients from healthy participants in the serum internal validation cohort

| | AUC | Odds Ratio | Specificity | Sensitivity | Accuracy |
|---|---|---|---|---|---|
| miR-18a | 0.67 (0.57 - 0.76) | 4.24 (2.09 - 8.57) | 0.44 (0.30 - 0.86) | 0.84 (0.49 - 0.95) | 0.78 (0.54 - 0.86) |
| miR-93 | 0.67 (0.58 - 0.75) | 3.66 (1.83 - 7.35) | 0.67 (0.49 - 0.95) | 0.64 (0.34 - 0.86) | 0.64 (0.44 - 0.79) |
| miR-146b | 0.58 (0.50 - 0.66) | 2.65 (1.27 - 5.53) | 0.74 (0.63 - 1.00) | 0.48 (0.19 - 0.62) | 0.52 (0.32 - 0.63) |
| miR-181b | 0.80 (0.74 - 0.85) | 15.62 (5.39 - 45.32) | 0.91 (0.74 - 1.00) | 0.62 (0.50 - 0.81) | 0.66 (0.58 - 0.81) |
| miR-335 | 0.66 (0.59 - 0.74) | 7.10 (2.45 - 20.57) | 0.91 (0.51 - 0.98) | 0.42 (0.36 - 0.81) | 0.50 (0.45 - 0.78) |
| Signature | 0.90 (0.85 - 0.94) | 20.69 (8.62 - 49.67) | 0.84 (0.77 - 1.00) | 0.80 (0.60 - 0.90) | 0.81 (0.66 - 0.88) |
| Abbreviation: AUC, area under the ROC curve. OR, odds ratio. | | | | | |

© 2021 Izumi D et al. *JAMA Network Open.*

**eTable 6.** Univariate and multivariate analysis using clinical factors and the circulating miRNA signature

| | **Univariate analysis** | | | **Multivariate analysis** | | |
|---|---|---|---|---|---|---|
| MicroRNA | OR (95% CI) | *P* value | | OR (95% CI) | *P* value | |
| Age | 2.22 (1.09 - 4.50) | **0.01** | | 1.03 (1.00 - 1.06) | 0.05 | |
| Gender | 1.32 (0.68 - 2.56) | 0.58 | | 0.51 (0.19 – 1.28) | 0.17 | |
| CEA | 0.36 (0.14 - 0.95) | 0.94 | | 0.99 (0.97 - 1.00) | 0.19 | |
| CA19-9 | 0.51 (0.19 - 1.35) | 0.77 | | 1.00 (1.00 – 1.01) | 0.02 | |
| Signature | 20.69 (8.62 - 49.67) | **<0.01** | | 2.96 (2.10 – 4.52) | **<0.01** | |
| Abbreviation: OR, odds ratio. CI, confidence interval | | | | | | |

© 2021 Izumi D et al. *JAMA Network Open.*

**eTable 7.** Analyses comparing our 5-circulating-miRNA signature with CEA and CA19-9 for non-invasive detection of gastric cancer (GC) across all stages and stage I in the prospective validation cohort.

| Comparison | Cohort | No. of participants | AUC | Accuracy | Sensitivity<br>Specificity | PPV<br>NPV | Difference |
|---|---|---|---|---|---|---|---|
| **miRNA signature for various patients** | | | | | | | |
| Gastric cancer | Kumamoto | 216 vs. 43 | 0.90 (0.85–0.94) | 0.81 (0.76–0.86) | 0.80 (0.60–0.90)<br>0.84 (0.77–1.00) | 0.96 (0.76–0.85)<br>0.46 (0.39–0.54) | |
| Gastric cancer | Kumamoto and Nagoya | 504 vs. 82 | 0.81 (0.76-0.85) | 0.68 (0.64-0.72) | 0.65 (0.61-0.69)<br>0.84 (0.76-0.91) | 0.96 (0.94-0.98)<br>0.28 (0.25-0.31) | |
| Colorectal cancer | Kumamoto | 38 vs. 43 | 0.54 (0.41–0.67) | 0.60 (0.51–0.70) | 0.39 (0.11–0.68)<br>0.79 (0.58–1.00) | 0.62 (0.45–0.80)<br>0.60 (0.53–0.67) | ***P*<0.05** |
| Colorectal cancer | GSE25609 | 20 vs. 21 | 0.58 (0.39-0.76) | 0.63 (0.56-0.73) | 0.25 (0.10-0.45)<br>1.00 (1.00-1.00) | 1.00 (1.00-1.00)<br>0.58 (0.54-0.66) | ***P*<0.05** |
| Pancreatic cancer | GSE85589 | 88 vs. 19 | 0.63 (0.48-0.77) | 0.71 (0.62-0.79) | 0.74 (0.64-0.82)<br>0.58 (0.37-0.79) | 0.89 (0.84-0.94)<br>0.32 (0.21-0.44) | ***P*<0.05** |
| Non-small cell lung cancer | GSE46729 | 24 vs. 24 | 0.48 (0.31-0.65) | 0.56 (0.48-0.65) | 0.96 (0.88-1.00)<br>0.17 (0.04-0.33) | 0.53 (0.49-0.59)<br>0.83 (0.33-1.00) | ***P*<0.05** |
| Breast cancer | GSE31309 | 48 vs. 57 | 0.61 (0.50-0.72) | 0.59 (0.51-0.67) | 0.90 (0.79-0.98)<br>0.33 (0.23-0.46) | 0.53 (0.48-0.58)<br>0.79 (0.64-0.94) | ***P*<0.05** |
| Ovarian cancer | GSE31568 | 15 vs. 70 | 0.56 (0.42-0.71) | 0.40 (0.32-0.48) | 1.00 (1.00-1.00)<br>0.27 (0.17-0.37) | 0.23 (0.21-0.25)<br>1.00 (1.00-1.00) | ***P*<0.05** |
| Stage I GC | Kumamoto | 84 vs. 43 | 0.89 (0.83–0.94) | 0.80 (0.72–0.87) | 0.77 (0.58–0.94)<br>0.84 (0.65–1.00) | 0.90 (0.84–0.96)<br>0.66 (0.57–0.76) | |
| **Comparing with current tumor markers** | | | | | | | |
| Signature | Kumamoto | 216 vs. 43 | 0.90 (0.85–0.94) | 0.81 (0.76–0.86) | 0.80 (0.60–0.90)<br>0.84 (0.77–1.00) | 0.96 (0.76–0.85)<br>0.46 (0.39–0.54) | |
| CEA (cutoff 3.4 ng/mL) | Kumamoto | 151 vs. 24 | 0.55 (0.40–0.70) | 0.77 (0.70–0.83) | 0.83 (0.34–0.97)<br>0.36 (0.14–0.86) | 0.90 (0.87–0.93)<br>0.24 (0.12–0.38) | ***P*<0.01** |
| CA19-9 (cutoff 37.0 U/mL) | Kumamoto | 148 vs. 21 | 0.56 (0.42–0.70) | 0.59 (0.51–0.66) | 0.59 (0.14–0.94)<br>0.58 (0.21–1.00) | 0.91 (0.87–0.96)<br>0.15 (0.10–0.21) | ***P*<0.01** |

Range values surrounded by brackets mean 95% confidence intervals. Abbreviations: AUC, area under the ROC curve. PPV, positive predictive value. NPV, negative predictive value. CEA, carcinoembryonic antigen. CA19-9, cancer antigen 19-9.

© 2021 Izumi D et al. *JAMA Network Open.*

**eTable 8.** Comparison of the performance of our 3-circulating-miRNA signature against CEA and CA19-9 for non-invasive detection of all-stage GC and stage I GC in the prospective validation cohort.

| | **3-miRNA signature** 216 (GC) vs 43 (Healty) | **3-miRNA signature (stage I)** 84 (GC) vs 43 (Healty) | **CEA (all stage)** 151 (GC) vs 24 (Healty) | **CA19-9 (all stage)** 148 (GC) vs 21 (Healty) |
|---|---|---|---|---|
| AUC | 0.86 (0.83–0.90) | 0.85 (0.79–0.91) | 0.65 (0.57–0.73) | 0.67 (0.59–0.76) |
| Odds Ratio | 18.2 (10.4–32.0) | 18.8 (8.89–39.9) | 2.83 (1.57–5.12) | 0.14 (0.07–0.27) |
| Accuracy | 0.80 (0.75–0.84) | 0.84 (0.79–0.89) | 0.63 (0.57–0.70) | 0.73 (0.67–0.79) |
| Sensitivity | 0.72 (0.65–0.78) | 0.72 (0.59–0.83) | 0.57 (0.46–0.68) | 0.56 (0.45–0.68) |
| Specificity | 0.88 (0.83–0.92) | 0.88 (0.83–0.92) | 0.68 (0.59–0.77) | 0.85 (0.78–0.91) |
| PPV | 0.86 (0.80–0.91) | 0.65 (0.56–0.75) | 0.57 (0.49–0.65) | 0.73 (0.63–0.83) |
| NPV | 0.75 (0.71–0.80) | 0.91 (0.88–0.94) | 0.69 (0.62–0.75) | 0.74 (0.69–0.79) |

Abbreviations: GC, gastric cancer. Healthy, healthy participants. CEA, carcinoembryonic antigen. CA19-9, cancer antigen 19-9. AUC, area under the ROC curve. PPV, positive predictive value. NPV, negative predictive value.

© 2021 Izumi D et al. *JAMA Network Open.*

**eTable 9.** Univariate and multivariate analyses comparing our 3-circulating-miRNA signature with age, sex, CEA, and CA19-9 for non-invasive detection of GC across all stages and stage I in the prospective validation cohort.

| | Prospective Validation Cohort (All Stages) | | | | | Prospective Validation Cohort (Stage I) | | | |
|---|---|---|---|---|---|---|---|---|---|
| | Univariable | | Multivariable | | | Univariable | | Multivariable | |
| | OR (95% CI) | *P* | OR (95% CI) | *P* | | OR (95% CI) | *P* | OR (95% CI) | *P* |
| 3-miR | 18.2 (10.4–32.0) | 1.83E-35 | 8.59 (4.56–18.2) | 8.36E-10 | | 18.8 (8.89–39.9) | 4.16E-18 | 4.25 (2.08–10.1) | 2.95E-4 |
| Age | 0.20 (0.12–0.33) | 8.88E-2 | 1.00 (0.97–1.03) | 8.47E-1 | | 0.17 (0.09–0.33) | 2.36E-1 | 1.03 (0.99–1.07) | 1.58E-1 |
| Sex | 1.33 (0.85–2.09) | 2.10E-1 | 0.82 (0.35–1.84) | 6.31E-1 | | 1.95 (0.96–3.99) | 5.62E-2 | 1.85 (0.50–7.98) | 3.74E-1 |
| CEA | 2.83 (1.57–5.12) | 5.90E-6 | 1.42 (1.09–1.98) | 2.64E-2 | | 3.37 (1.35–8.38) | 1.20E-2 | 2.01 (1.27–3.36) | 4.41E-3 |
| CA19-9 | 0.14 (0.07–0.27) | 3.37E-1 | 1.00 (0.99–1.02) | 2.24E-1 | | 0.07 (0.03–0.18) | 1.44E-4 | 0.86 (0.77–0.94) | 2.52E-3 |

Abbreviations: OR, odds ratio, CEA, carcinoembryonic antigen. CA19-9, cancer antigen 19-9.
Healthy participants 173, patients with all stages GC 176 and patients with stage I GC 54.

© 2021 Izumi D et al. *JAMA Network Open.*

**eTable 10.** Results of cost-effectiveness analysis

| | **Non-invasive screening program** | **No-screening** |
|---|---|---|
| Cohort size | 100000 | 100000 |
| Total number of cancer patients in the cohort | 5000 | 5000 |
| Compliance | 45% | 10% |
| Stage of diagnosis (Stage 1; 2; 3; 4) | 17.57%; 21.96%; 34.74%;25.73% | 11.50%; 19.47%; 42.71%; 26.33% |
| Average cost of diagnosis | CNY 447.1 | CNY 48.7 |
| **Results of cost-effectiveness analysis (CEA)** | | |
| Total cost | 1172.2M | 1115.1M |
| Total QALY | 2337.0K | 2333.5K |
| Cost difference | 570.1 | |
| Effect difference | 0.035 | |
| Cost of saving 1 QALY | CNY 16162.5/QALY | |

© 2021 Izumi D et al. *JAMA Network Open.*

**eTable 11.** Clinical assumptions of the hypothetical cohort used for the cost effectiveness analysis

| | Value | Ref. |
|---|---|---|
| **Cost** | | |
| miRNA assay | 300 | Estimated |
| Endoscopy | 304 | Estimated using internal records |
| Biopsy | 108 | Estimated using internal records |
| Stage 1 treatment | 62205 | Annual cost Yang et al. Chinese Journal of Cancer Research 2018 (PMID: 30210224) |
| Stage 2 treatment | 42231 | |
| Stage 3 treatment | 49983 | |
| Stage 4 treatment | 36865 | |
| Follow-up examinations | 700 | Estimated |
| Staging Investigation | 1500 | Estimated |
| | | |
| **Cancer cases in high risk population** | 5% | Estimated |
| **Portion by stage** | | |
| Stage 1 | 11.50% | Yang et al. Chinese Journal of Cancer Research 2018 (PMID: 30210224) |
| Stage 2 | 19.47% | |
| Stage 3 | 42.71% | |
| Stage 4 | 26.33% | |
| **Incidence of cancer** | (1/100000) | |
| 50-54 | 29.31 | Yang et al. Chinese Journal of Cancer Research 2018 (PMID: 30046223) |
| 55-59 | 54.36 | |
| 60-64 | 87.09 | |
| 65-69 | 122.39 | |
| 70-74 | 156.03 | |
| >75 | 513.72 | |
| **5-yr recurrence rate of cancer by stage** | | |
| Stage 1 | 2.19% | Xu et al. Cancer Medicine 2016 (PMID: 32420703) |
| Stage 2 | 8.12% | |
| Stage 3 | 28.35% | |
| **Utility Values** | | |
| Stage 1 | 0.88 | Zhou el at. PLoS ONE 2013 (PMID: 24386314) |
| Stage 2 | 0.86 | |
| Stage 3 | 0.77 | |
| Stage 4 | 0.68 | |
| Cured | 0.88 | Estimated |

© 2021 Izumi D et al. *JAMA Network Open.*